THE EFFECT OF NON-SINUSOIDAL IMPRESSED VOLTAGES ON A. C. SERVO MOTORS

CHARLES W. BUSEY

Library
U. S. Naval Postgraduate School
Monterey, California

1-26

SES - SERVO-MOTORS
SIN - SINUSOIDAL
VOL - VOLTAGE

THE EFFE

Perry G. Davis BOOKBINDING
2216 CLEMENT STREET San Francisco 21, Calif. BA. 1-6352

DIRECTIONS FOR BINDING

BUCKRAM
COLOR NO. 8854

FABRIKOID
COLOR

LEATHER
COLOR

Letter in Gold

OTHER INSTRUCTIONS

LETTERING ON BACK
TO BE EXACTLY AS
PRINTED HERE.

BUSEY

1955

THESIS
B92

Letter on front cover:

THE EFFECT OF NON-SINUSOIDAL IMPRESSED
VOLTAGES ON A. C. SERVO MOTORS

CHARLES W. BUSEY

THE EFFECT OF NON-SINUSOIDAL IMPRESSED VOLTAGES
ON
A. C. SERVO MOTORS

by

Charles Webb Busey

Lieutenant, United States Navy

and

William Russell Bartow

Lieutenant, United States Navy

Submitted in partial fulfillment
of the requirements
for the degree of
MASTER OF SCIENCE
IN
ELECTRICAL ENGINEERING

United States Naval Postgraduate School
Monterey, California

1955

Thesis
B92

Library
U. S. Naval Postgraduate School
Monterey, California

This work is accepted as fulfilling
the thesis requirements for the degree of

MASTER OF SCIENCE
IN
ELECTRICAL ENGINEERING

from the
United States Naval Postgraduate School

PREFACE

In response to a suggestion by the Bureau of Ships, Navy Department, Washington, D. C., investigation as to the effects of non-sinusoidal impressed voltages on the operation of alternating current servo motors was undertaken in October 1954 at the Electrical Engineering Laboratory, U.S. Naval Postgraduate School, Monterey, California.

Inter-related with the effects of non-sinusoidal impressed voltages are the effects of space harmonics of magneto-motive force, the latter producing such phenomena as asynchronous crawling and sub-synchronous locking. Bearing this in mind, an effort was made to detect adverse effects upon the operation of several two-phase induction servo motors which might be attributable to either time or space harmonics, or possibly a combination of the two. The motors tested were standard production models except where one modification was made in an endeavor to specifically create an unfavorable design situation.

The results of this investigation indicated that wave form, balanced or unbalanced, had no seriously adverse effect upon the torque-speed characteristics of the motors tested. This might have been anticipated of production models where design features would certainly tend to eliminate or minimize such effects.

The writers acknowledge and deeply appreciate the

assistance and encouragement given by Professor W. A. Stein, U. S. Naval Postgraduate School, throughout the entire period of this investigation.

TABLE OF CONTENTS

Item — Page

Certificate of Approval i

Preface ii

List of Illustrations v

Table of Symbols and Abbreviations vii

Chapter I Introduction 1

Chapter II Theoretical Analysis
1. Non-sinusoidal waves 4
2. Time harmonics 4
3. Space harmonics 5
4. Harmonics in practical systems 7
5. Development of torque 7
6. Time-harmonic torques 8
7. Heating effects of non-sinusoidal waves 13
8. Space-harmonic torques 14
9. Unbalanced complex waves 14
10. Summary of theory 17

Chapter III Investigative Proceedure and Results
1. Testing equipment 19
2. Circuitry and instrumentation 19
3. Selection of motors to be tested 22
4. Proposals 23
5. General precautions 23
6. Sinusoidal time-harmonic test data 24
7. Space-harmonic test data 25
8. Unbalanced time-harmonic test data 26
9. Appraisal of test data 28

Chapter IV Conclusions 29

Bibliography 31

LIST OF ILLUSTRATIONS

Illustration		Page
1.	Schematic diagram of circuitry for early phases of investigation	32
2.	Schematic diagram of frequency control and oscilloscope triggering circuits	33
3.	Photograph of harmonic generator	34
4.	Frequency tripler circuit	35
5.	Photograph of dynamometer and temperature control	36
6.	Temperature characteristics of Ketay motor	37
7.	Temperature characteristics of Kearfoot motor	38
8.	Current oscillograms showing effects of saturation for 400/1200 cps investigation	39
9.	Current oscillograms of rated and sub-rated currents for 400/1200 cps investigation	40
10.	Family of torque-speed curves for Ketay motor	41
11.	Stall torque versus control voltage for Ketay motor	42
12.	Ketay torque-speed curves for complex impressed voltages	43
13.	Cutaway photograph of Kearfoot motor	44
14.	Rated torque-speed curve of Kearfoot motor	45

Illustration		Page
15.	Kearfoot torque-speed curve for 400/1200 cps investigation	46
16.	Schematic diagram of wattmeter transfer switch	47
17.	Photograph of frequency tripler set-up	48

TABLE OF SYMBOLS AND ABBREVIATIONS

(Listed Alphabetically)

α - Space angle

a.c. - Alternating-Current

d.c. - Direct-Current

cps - Cycles per second

f_n - Frequency of Nth harmonic

H - Magnetic intensity

H_{Cn} - Magnetic intensity of Nth harmonic of control phase

H_{Rn} - Magnetic intensity of Nth harmonic of reference phase

K - Any constant multiplier

P - Number of poles

R_1 - Primary ohmic resistance

R_2 - Secondary ohmic resistance referred to primary terms

rms - Root-mean-square

rpm - Revolutions per minute

s - Slip

s_n - Slip in terms of Nth harmonic synchronous speed

T_{MAX} - Maximum torque per phase

T_n - Torque of Nth harmonic per phase

T_{ST} - Stall torque per phase

V_n - Effective (rms) value of Nth harmonic voltage per phase

ω - Angular velocity

ωt - Time angle

x_1 - Primary leakage reactance per phase

x_2 - Secondary leakage reactance per phase referred to primary terms

$y_{\square}$ - Instantaneous height of rectangular wave

$y_{\triangle}$ - Instantaneous height of triangular wave

$\triangleq$ - Equal by definition

CHAPTER I

INTRODUCTION

Automation is a newly coined word tending to describe the modern trend toward greater and greater application of automatic control. A system by which automatic control is obtained is generally referred to as a servomechanism, and it may be one or a combination of several mechanical, hydraulic, pneumatic, or electrical components.

The two-phase induction motor is an electrical component widely used in control systems. For such application, characteristics such as bi-directional control, linear variation of torque with speed, linear variation of torque with amplitude of signal, and high starting torque are particularly desirable, and much study has been devoted to the development of two-phase induction motors that possess these characteristics. A motor so designed is commonly referred to as a servo motor.

The classical analysis of the operation and characteristics of the induction motor is based upon the assumption that the impressed voltages, the air gap and rotor fluxes, and the primary and secondary currents are all sinusoidal. Using this assumption, Professor Koopman /7/* showed that the torque versus speed curve is essentially linear, and

---

* Numerals in brackets refer to bibliography. See page 28.

that the torque versus control voltage is precisely linear at stall. In practice, however, these assumptions are rarely valid, and the effect this deviation may have on the theoretical operation of the servo motor therefore becomes of vital interest to those charged with the specification, design, and development of servomechanisms.

The purpose of this investigation was to determine the effect of non-sinusoidal voltages upon the theoretical torque-speed characteristics of the servo motor. A general investigation would have been desirable, but such investigation would have required the design features of the motors under test to be variable in order to show the effects of coil pitch, distribution of winding, skew of rotor slots, and rotor resistance. Unfortunately, access to such motors could not be had, and consequently the investigation was limited to production models in which the designers had presumably utilized all means at their disposal to adjust the motor parameters so as to provide optimum characteristics. Thus the investigation became one to determine effects upon a few particular, but representative, models rather than an investigation of comprehensive scope.

The plan of procedure was roughly divided into two parts. In the first part, families of torque versus speed curves were obtained for balanced sinusoidal impressed voltages of various magnitudes and frequencies, and for balanced non-sinusoidal voltages of known harmonic content. The torque

versus speed characteristics of the non-sinusoidal impressed voltages should theoretically be the same as the resultant torque obtained by superposition of the individual harmonic torques.

The second part of the plan was to force sinusoidal currents of harmonic frequencies through one phase winding while maintaining current in the other phase winding sinusoidal and of fundamental frequency. It was recognized that no torque would be produced by time harmonics in this instance, but the effect due to a possible combination of time and space harmonics was not obvious; indeed, it was intuitively felt that a torque would exist irrespective of the negative indication given by the theoretical analysis of Chapter II.

The test results of both phases of the investigation tended to verify in a most convincing manner, the theoretical predictions pertaining to the effects upon the operating characteristics of the motors tested.

CHAPTER II

THEORETICAL ANALYSIS

1. Non-sinusoidal waves.

Fourier demonstrated how certain periodic functions could be analyzed into an infinite series of sinusoidal functions of increasing frequency. The lowest frequency present in such an analysis is generally taken as the reference, or fundamental, while the higher order frequencies are termed harmonics.* As examples, the Fourier analysis of the rectangular wave is:

$$y_{\square} = A_1 \sin\alpha + \frac{A_1}{3}\sin 3\alpha + \frac{A_1}{5}\sin 5\alpha - - - -$$

where $A_1 \triangleq \frac{4}{\pi}$ times height of rectangle

and the analysis of the triangular wave is

$$y_{\triangle} = \frac{8A_1}{\pi^2}\left(\sin\alpha - \frac{1}{3^2}\sin 3\alpha + \frac{1}{5^2}\sin 5\alpha - - - -\right)$$

where $A_1 \triangleq$ height of triangle

Thus these non-sinusoidal waves may be considered to be the sum of their individual sinusoidal components.

2. Time harmonics.

The harmonics of the impressed voltages and/or currents are called time harmonics. If equal non-sinusoidal currents flow in each winding of the primary of a two-phase induction

---

* In some analyses, such as Kron's paper on Induction Motor Slot Combinations, it may be convenient to choose as reference some frequency of lower order than the lowest frequency actually present.

motor having sinusoidal space distribution of air gap flux, then each time harmonic of the current will establish its own rotating magnetic field, and the field of the Nth harmonic will rotate at a speed N times as fast as the field of the fundamental.

3. Space harmonics.

The magnetic intensity of a field induced by a current flowing in a closed coil acts normal to the plane of the coil and is uniform everywhere within the closed path. Where the current varies sinusoidally with time, the resultant magnetic intensity will also vary with time; yet, at any particular instant, the intensity will be uniform everywhere within the closed path of the coil. Suppose Fig. 1a represents a sectional view of a single turn coil. If the coil is stationary, as it would be if it were part of the stator winding of an induction motor, and if the current through the coil varies sinusoidally with time, then the H vector (magnetic intensity) will vary in magnitude with time as the current in the coil varies. This type of variation is referred to as a standing wave, and in this instance the wave shape of the H vector would be rectangular. The Fourier analysis of a rectangular wave was given in paragraph 1.

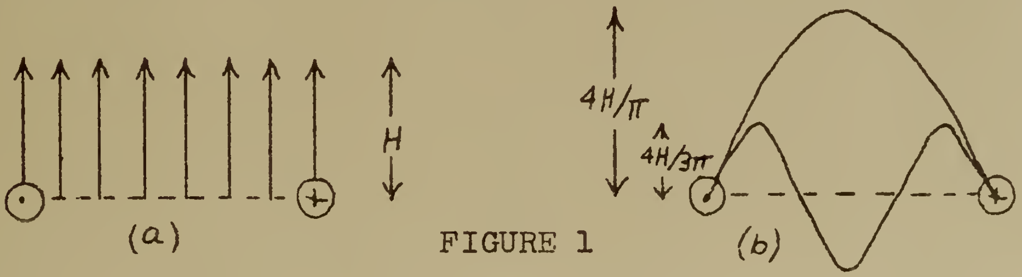

(a) FIGURE 1 (b)

Thus a standing rectangular wave may be analyzed as being composed of an infinite series of standing sinusoidal waves. Fig. 1b depicts the fundamental and third-space harmonic of the square wave of Fig. 1a.

A standing sinusoidal wave may further be analyzed as being the equivalent of two sinusoidal waves of the same frequency but of half magnitude and travelling in opposite directions. This, of course, applies to each harmonic of the standing rectangular wave, and in this manner, the stationary but time variant H vector may be resolved into an infinite number of travelling components.

Suppose that the fundamental of Fig. 1b represents a sinusoidal distribution of flux from one pole, then it is obvious that the third harmonic would be analogous to the sinusoidal distribution of flux from three poles and the Nth from N poles. Since all travelling waves move through one pole pitch in the same increment of time, the Nth harmonic must require N times as long to make one revolution of the stator as compared to the fundamental wave. Herein lie the basic differences between time and space harmonics. Whereas the Nth time harmonic of current produces a flux pattern of the same number of magnetic poles as the fundamental, but rotating at a synchronous speed N times that of the fundamental; the Nth space harmonic of flux produces a flux pattern having N times the number of fundamental poles but rotating at a synchronous speed $\frac{1}{N}$ times that of the funda-

mental. As an illustration, consider a 60 cycle, two-phase, two-pole induction motor. The third time harmonic of this motor would have a two-pole flux pattern rotating at 10,800 rpm, while the third space harmonic of the same motor would have a six-pole flux pattern rotating at 1200 rpm.

4. Harmonics in practical systems.

Practical control systems contain various non-linear elements such as iron-core inductances, phase-shifting networks, and electronic amplifiers that tend to distort the voltages and currents before they reach the windings of the servo motor. These distortions produce time harmonics. On the other hand, the types and relative magnitudes of space harmonics that may be present in the stator and/or the rotor are limited by the design features of the motor. Some of these design features are: distribution of stator windings, coil pitch, skew and number of rotor slots, and rotor resistance. Actually, there is an infinite number of combinations of the various types of harmonics that can combine to produce rotating magnetic fields in stator and rotor having synchronous speeds different from the fundamental synchronous speed /8/. Obviously, the effect of these so-called "parasitic" fields, when present, will depend upon their magnitude relative to the fundamental field. Fortunately, only the lower order harmonics are significant.

5. Development of torque.

The analysis of the induction motor had little meaning

until Blondel introduced his equivalent circuit. Additional impetus to ready analysis under all conditions of load was given by the circle diagram as proposed by Behrend /2/. With the tools provided by these men, it was easy to derive the approximate mathematical equations for torque, stall torque, maximum torque, and slip at maximum torque as follows:*/9/

$$T_n = \frac{PV_n^2}{4\pi f_n} \times \frac{sR_2}{(sR_1 + R_2)^2 + s^2(x_1 + x_2)^2}$$

$$T_{n_{st}} = \frac{PV_n^2}{4\pi f_n} \times \frac{R_2}{(R_1 + R_2)^2 + (x_1 + x_2)^2}$$

$$T_{n_{max}} = \frac{PV_n^2}{4\pi f_n} \times \frac{1}{2[R_1 + \sqrt{R_1^2 + (x_1 + x_2)^2}}$$

$$S_{n_{max}} = \frac{R_2}{[R_1 + (x_1 + x_2)^2]^{1/2}}$$

These equations apply to any time harmonic of order N provided there is a rotating flux in the primary and an induced current in the secondary, both of frequency N. It must be recognized that the terms primary and secondary as used here apply jointly to rotor and stator. Thus any pair of fluxes, regardless of source, that combine to produce a rotating flux will react upon a secondary current of the same frequency to produce a torque: and, contingent upon the direction of rotation of the flux, these torques can be either positive or negative.

6. Time-harmonic torques.

As previously stated, the servo motor is a two-phase

---

* See table of abbreviations for meaning of symbols.

induction motor with a high-resistance rotor. In this respect it differs from the ordinary industrial induction motor that obtains maximum torque at a speed within a few percent of synchronous speed. The large value of R_2 of the servo motor causes the maximum torque to occur outside of the normal operating range of the motor as indicated by the torque-speed curve shown in Fig. 2. This curve clearly illustrates how the relatively high value of R_2 provides the desirable characteristics of near-linear torque-speed relationship and stability throughout the normal operating range between zero and unity slip.

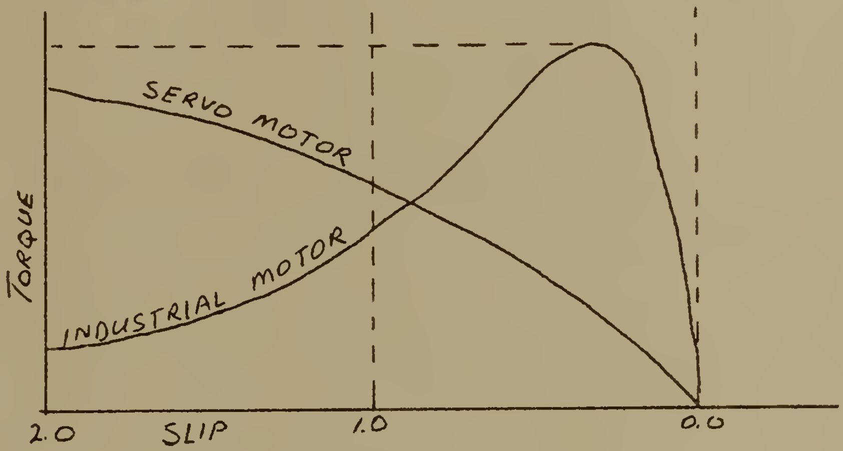

FIGURE 2

Consider the equation for stall torque of fundamental frequency as given in paragraph 5 above, and repeated here:

$$T_{ST} = \left(\frac{p V_m^2}{4\pi f_m}\right)\left[\frac{R_2}{(R_1+R_2)^2+(x_1+x_2)^2}\right]$$

It is difficult to say how the bracketed term will vary with increasing frequency for any particular motor, but the effective values of R_1 and R_2 will probably increase slightly

due to increased skin effect while the values of x will increase linearly. The servo motor being inherently a high resistance machine, the ratio of $(R_1+R_2)/(x_1+x_2)$ will probably exceed 20 times the ratio of these parameters for an ordinary induction motor. The effect of increased reactance is consequently very, very much less in the servo motor. The term in parentheses, however, will vary inversely with the frequency and directly as the square of the impressed voltage. Disregarding the bracketed term, one could expect that the torque developed by an impressed voltage of one-third magnitude and three times frequency would be approximately

$$T_{ST} = \frac{P}{4\pi}\,\frac{(V_1/3)^2}{3f_1} = \frac{PV_1}{4\pi f_1}\cdot\frac{1}{27}$$

or $\frac{1}{27}$ times the torque developed by voltage V_1 at frequency f_1. This situation obtains when considering the third time harmonic of a rectangular wave where V_1 and f_1 would apply to fundamental values of impressed voltage and frequency.

When considering the probable effect of the third-time harmonic of a triangular wave, one must again refer to the Fourier analysis of that wave where it is seen that the magnitude of the third harmonic is one ninth of the fundamental. The stall torque of the third harmonic alone would then be, approximately

$$T_{ST_3} = \frac{P}{4\pi}\,\frac{(V_1/9)^2}{3f_1} = \frac{PV_1^2}{4\pi f_1}\cdot\frac{1}{243}$$

or $\frac{1}{243}$ times the torque developed by the fundamental, and, as with the rectangular wave, the algebraic sign would be negative.

In regard to the algebraic sign of the third time harmonic torque, consider the following analysis: Let $\left[\sin\alpha + \frac{1}{3}\sin 3\alpha + \frac{1}{5}\sin 5\alpha - - - - - \right]$ represent the space-variant terms of the H vector of the reference winding; $\left[\sin(\alpha + \pi/2) + \frac{1}{3}\sin 3(\alpha + \pi/2) + \frac{1}{5}\sin 5(\alpha + \pi/2) - - - - \right]$ represent the space-variant terms of the H vector of the control winding; $\left[I_{R_1}\cos\omega t + I_{R_3}\cos 3\omega t - - - - \right]$ represent the current flowing in the reference winding; and $\left[I_{C_1}\cos(\omega t + \pi/2) + I_{C_3}\cos 3(\omega t + \pi/2) - - - - \right]$ represent the current flowing in the control winding. Now if all space harmonic terms except the fundamental are dropped, meaning that consideration is only being taken of the space fundamental, and since space distribution of time harmonics does not vary with the order of the harmonics, the respective H vectors may be expressed as

$$H_R = K\left[I_{R_1}\cos\omega t + I_{R_3}\cos 3\omega t\right]\sin\alpha$$

$$H_c = K\left[I_{C_1}\cos(\omega t + \pi/2) + I_{C_3}\cos 3(\omega t + \pi/2)\right]\sin(\alpha + \pi/2)$$

whence

$$H_R = K\left[I_{R_1}\sin\alpha\cos\omega t + I_{R_3}\sin\alpha\cos 3\omega t\right]$$

$$= \frac{KI_{R_1}}{2}\left[\sin(\alpha - \omega t) + \sin(\alpha + \omega t)\right]$$

$$+ \frac{KI_{R_3}}{2}\left[\sin(\alpha - 3\omega t) + \sin(\alpha + 3\omega t)\right]$$

and

$$H_C = KI_{C_1}\left[\sin(\alpha+\pi/2)\cos(\omega t+\pi/2)\right]$$

$$+KI_{C_3}\left[\sin(\alpha+\pi/2)\cos 3(\omega t+\pi/2)\right]$$

$$=\frac{KI_{C_1}}{2}\left[\sin(\alpha+\pi/2-\omega t-\pi/2)+\sin(\alpha+\pi/2+\omega t+\pi/2)\right]$$

$$+\frac{KI_{C_3}}{2}\left[\sin(\alpha+\pi/2-3\omega t-3\pi/2)+\sin(\alpha+\pi/2+3\omega t+3\pi/2)\right]$$

$$=\frac{KI_{C_1}}{2}\left[\sin(\alpha-\omega t)-\sin(\alpha+\omega t)\right]$$

$$+\frac{KI_{C_3}}{2}\left[-\sin(\alpha-3\omega t)+\sin(\alpha+3\omega t)\right]$$

The net flux in the stator is of course the resultant of the fluxes in the two windings, or

$$H = H_R + H_C$$

$$=\left[K\left(\frac{I_R+I_{C_1}}{2}\right)\sin(\alpha-\omega t)+K\left(\frac{I_{R_1}-I_{C_1}}{2}\right)\sin(\alpha+\omega t)\right]$$

$$+\left[K\left(\frac{I_{R3}+I_{C3}}{2}\right)\sin(\alpha-3\omega t)+K\left(\frac{I_{R3}-I_{C3}}{2}\right)\sin(\alpha+3\omega t)\right]$$

When the currents flowing in the respective windings are balanced, $I_{R_1}=I_{C_1}$ and $I_{R_3}=I_{C_3}$ Therefore,

$$H=K\left(\frac{I_{R_1}+I_{C_1}}{2}\right)\sin(\alpha-\omega t)+K\left(\frac{I_{R_3}+I_{C_3}}{2}\right)\sin(\alpha+3\omega t)]$$

Here the first sine term is the fundamental rotating time flux and the second sine term is the third time-harmonic rotating flux. Notice that the latter varies negatively with time relative to the fundamental. Thus the algebraic sign of the third time-harmonic rotating flux and consequently the third time-harmonic torque is negative. In like manner it could be shown that the sign of the time-harmonic torques of higher orders will alternate positive and negative.

7. Heating effects of non-sinusoidal waves.

Probably the most important single design consideration involved in the rating of a servo motor is the allowable temperature rise which is a function of the heating effect, or rms value, of the impressed voltage. When equivalent rms values of impressed waves are maintained, the magnitude of the fundamental frequency component of a non-sinusoidal wave is always less than the magnitude of a pure sinusoid of that frequency. As examples, the ratio of the maximum value of the fundamental component of a square wave to the maximum value of a pure sinusoid of same rms value as the square wave would be $4/\pi\sqrt{2}$, and the ratio of maximum values of fundamental components of triangular wave and a pure sinusoid would be $8\sqrt{3}/\pi^2\sqrt{2}$. Since the torque varies as the square of the impressed voltage, the fundamental torque of these two non-sinusoidal waves would be 81 and 98.5 percent of the torque that would be developed by a pure sinusoid.

This reduction in torque is in addition to the decrease resulting from negative third time-harmonic torque as discussed in paragraph 7.

8. Space-harmonic torques.

The torque-producing combinations of space harmonics that may exist in any particular induction motor are limited by the design features of the specific motor. Some of these design features tend to minimize the effects of the higher order space harmonics while others tend to eliminate them completely from either the primary or secondary. Whether a motor is "usable" or not is an indication of how effectively these design features have been utilized. Kron /8/ gives a comprehensive treatment of torques produced by space harmonics of stator and rotor and the effects of same in his paper "Induction Motor Slot Combinations". The subject is much too complex to be reduced or summarized for inclusion here. Suffice it to say that in all usable induction motors, the space-harmonic torques have been sufficiently minimized by proper design technique so as to render their effects negligible.

9. Unbalanced complex waves.

Until now, all analysis of the effects upon the net torque of a servo motor have been analyzed with regard to balanced voltages, whether sinusoidal or complex. Quite commonly, however, the control voltage is very small and must be amplified and shifted in phase in order to obtain

the proper magnitude and phase relationship relative to the reference winding in order to obtain the torque desired from the servo motor. The result of this amplification and phase shifting is frequently to introduce time harmonics into the control winding voltage that do not exist in the reference winding voltage. The question naturally arises, will these unbalanced voltages cause parasitic torques that will introduce irregularities in the torque-speed curve?

Anyone would readily say that there could be no time-harmonic torque resulting from a third-time harmonic in the control winding and a fundamental-time harmonic in the reference winding, but is it intuitively evident that there would not be a time-space combination that could possibly produce a parasitic torque? It was not so evident to the authors because it could be reasoned that the third-space harmonic of the third-time harmonic would have the same synchronous speed as the fundamental.

The mathematical analysis of this situation follows:

Let

$$H_R = KI_R \cos\omega t\left[\sin\alpha + \tfrac{1}{3}\sin 3\alpha + \tfrac{1}{5}\sin 5\alpha ----\right]$$

$$H_c = KI_c \cos 3(\omega t + \pi/2)\left[\sin(\alpha + \pi/2) + \tfrac{1}{3}\sin(\alpha + \pi/2) + ----\right]$$

then

$$H_R = KI_R \sin\alpha\cos\omega t + \frac{KI_R}{3}\sin 3\alpha\cos\omega t + \frac{KI_R}{5}\sin 5\alpha\cos\omega t$$

$$H_R = \frac{KI_R}{2}\left[\sin(\alpha-\omega t)+\sin(\alpha+\omega t)\right]$$

$$+\frac{KI_R}{6}\left[\sin(3\alpha-\omega t)+\sin(3\alpha+\omega t)\right]$$

$$+\frac{KI_R}{10}\left[\sin(5\alpha-\omega t)+\sin(5\alpha+\omega t)\right]$$

and

$$H_c = \frac{KI_c}{2}\left[\sin\left(\alpha+\pi/2-3\omega t-3\pi/2\right)+\sin\left(\alpha+\pi/2+3\omega t+3\pi/2\right)\right]$$

$$+\frac{KI_c}{6}\left[\sin\left(3\alpha+3\pi/2-3\omega t-3\pi/2\right)+\sin\left(3\alpha+3\pi/2+3\omega t+3\pi/2\right)\right]$$

$$+\frac{KI_c}{10}\left[\sin\left(5\alpha+5\pi/2-3\omega t-3\pi/2\right)+\sin\left(5\alpha+5\pi/2+3\omega t+3\pi/2\right)\right]$$

$$H_c = \frac{KI_c}{2}\left[-\sin(\alpha-3\omega t)+\sin(\alpha+3\omega t)\right]$$

$$+\frac{KI_c}{6}\left[\sin(3\alpha-3\omega t)-\sin(3\alpha+3\omega t)\right]$$

$$+\frac{KI_c}{10}\left[-\sin(5\alpha-3\omega t)+\sin(5\alpha+3\omega t)\right]$$

It can now be seen that through the fifth space harmonic of each impressed current there will be no cancellation of any of the positively and negatively rotating fluxes so as to give a net torque. Considering only the third-space of the third-time of the control winding gives the following terms:

$$H_{c_3} = \frac{KI_{c3}}{6}\left[\sin 3(\alpha-\omega t)-\sin 3(\alpha+\omega t)\right]$$

Even though the terms of the above expression have the same synchronous speed as the fundamental H_{r1} waves, the addition

of these two H waves gives

$$\begin{aligned} H_{R_1} + H_{C_3} &= \frac{KI_R}{2}\left[\sin(\alpha-\omega t) + \sin(\alpha+\omega t)\right] \\ &\quad + \frac{KI_C}{6}\left[\sin 3(\alpha-\omega t) - \sin 3(\alpha+\omega t)\right] \\ &= \left[\frac{KI_R}{2}\sin(\alpha-\omega t) + \frac{KI_C}{6}\sin 3(\alpha-3\omega t)\right] \\ &\quad + \left[\frac{KI_R}{2}\sin(\alpha+\omega t) - \frac{KI_C}{6}\sin 3(\alpha+\omega t)\right] \end{aligned}$$

where the first bracketed term is the forward-rotating resultant H vector and the second bracketed term is the backward-rotating resultant H vector.

These vectors are identical except for the 180 degree phase reversal of the third-harmonic term. Since the torque developed is independent of the phase relationship of the components of a complex wave, the forward and backward-rotating complex H vectors given above will produce equal and opposite torques, or a zero net rotating torque. These oppositely rotating torques would of course be equivalent to a standing or pulsating torque and could cause serious vibrations.

10. Summary of theory.

Summarizing the above theoretical considerations, it may be stated that:

a) Time harmonics will reduce the net output torque if heating effects are maintained constant. This reduction in torque, however, would probably never exceed 25 percent of rated sinusoidal torque even under the most adverse conditions encountered in practice.

b) Space harmonics would, if present, render a servo motor useless as a linearly responsive control device; however, space harmonics may be eliminated or minimized by careful design techniques.

c) Unbalanced harmonic content would reduce output for a given temperature rise - as in (a) above - but would not adversely effect the shape of the torque-speed curve.

CHAPTER III

INVESTIGATIVE PROCEEDURE AND RESULTS

1. Testing equipment.

All equipment used during this investigation was regular laboratory equipment available to students of the Electrical Engineering Department of the U. S. Naval Postgraduate School. Included were the following items:

a) A gang motor-generator unit having a d.c. driving motor and separate a.c. generators of frequencies ω , 2ω , 3ω, 5ω, and 7ω. The rated fundamental frequency of this unit is 60 cycles at 3600 rpm, but variations are available by virtue of the variable-speed d.c. motor drive.

b) A General Radio type 736-A wave analyzer capable of measurement of individual periodic components of a complex wave with a range of 30-300v; 20-16,500 cycles.

c) A special dynamometer developed specifically for testing small motors by S. H. Van Wambeck and W. A. Stein /13/.

d) Oscilloscopes, motors, thermo-couples, photographic equipment, etc., as required for instrumentation.

2. Circuitry and instrumentation.

a) Two-phase voltage source: The balanced two-phase voltages used in this investigation were obtained from the three-phase generators by connecting two of the three phases as in a wye connection. This provided a voltage 1.73 times phase voltage and displaced 90 degrees from the remaining

phase voltage. Four leads were brought from the generator terminal panel to variacs where the voltages could be varied individually as required. (See illustration 1)

b) Frequency control: The speed of the d.c. drive motor for the generators was controlled manually through a Ward-Leonard system. The output frequency was compared to an audio-oscillator signal by means of a Lissajou figure on a cathode ray oscilloscope. (See illustration 2)

c) Harmonic displacement: The individual generators of the gang harmonic-generator were mounted on cradles that could be rotated by means of a worm gear and locked at any chosen displacement relative to the fundamental-frequency generator. (See illustration 3) Displacement of the various voltages was indicated by a cathode-ray oscilloscope that was triggered by a signal from the fundamental-frequency generator. This triggering circuit is shown in illustration 2.

d) 1200 cycle voltage: The 1200 cycle voltage used in the time-space investigation was obtained by a tripler circuit (see illustration 4) that was essentially an open delta connection. The voltage at open delta was only 15 volts with five percent fundamental even though the phase voltages were taken through variacs to obtain optimum balance. This voltage was purified by passing through a band-pass filter that reduced the 400 cycle content to less than one percent before amplification to final value. Three hundred sixty

degree phase shift of this voltage relative to the 400 cycle voltage was obtained by means of a synchro transmitter.

e) Temperature rise: Motor case temperature above ambient was measured with a thermo couple and galvanometer calibrated to indicate one degree Centigrade for each graduation of scale. Ambient temperature was measured with a mercury thermometer suspended directly above the cold junction of the thermocouple. Temperature was controlled by means of a variable speed blower that was shut off during all balance readings of the dynamometer. This set-up may be seen in illustration 5.

f) Voltage, current, and power measurement: Illustrations 1 and 2 show the meter arrangement used for measurement of voltage, current, and power during the early phases of the investigation. In all instances, the meter load was determined and recorded prior to recording of of test data. Only one wattmeter was used, but compensating series and shunt resistances were included in the switching circuit so as to maintain balanced instrumentation load at all times. In the later phases of the investigation, this metering circuit was abandoned in favor of the following arrangement. A one ohm carbon pile resistance was inserted in series with each phase winding. The phase voltages and currents were then metered by a single vacuum tube voltmeter through the rotary selector switch, the current being equal to the voltage drop across the carbon pile resistor. The current wave

shape was observed on a cathode-ray oscilloscope and analyzed by the wave analyzer to assist in maintaining as pure a sinusoid as feasible so as to preserve the conditions of the theoretical analysis. See illustration 4 for schematic diagram of this circuitry.

3. Selection of motors to be tested.

It was originally intended to test only 60 cycle motors because of the rating of the harmonic generator. The Bureau of Ships provided several prototype motors for this purpose. Study of the winding data of these motors, however, indicated that all were wound with distributed windings that practically eliminated the third and fifth space harmonics from the stator. This of course made them useless for investigation of space harmonics but ideally suited for investigation of time harmonics.

An investigation of the winding arrangement of the Kearfoot, type R 111-2-B, 400 cycle servo motor showed that it had unity pitch factor and distribution factor, and, as shown below in figure 3, the variation of air gap permeance could

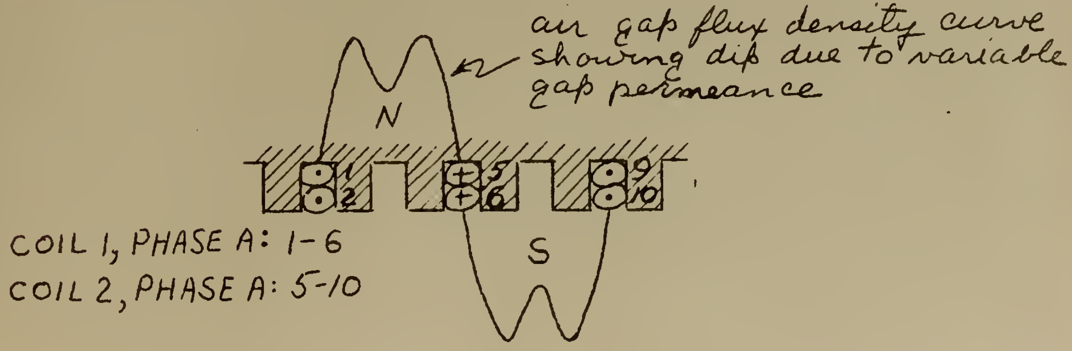
air gap flux density curve showing dip due to variable gap permeance
N
1
2
5
6
9
10
S
COIL 1, PHASE A: 1-6
COIL 2, PHASE A: 5-10

FIGURE 3

be expected to introduce a decided third harmonic in the air gap flux density. All of these design features suggested that the stator would be ideal for an investigation of the effects of space harmonics. The problem of the frequency could be solved by running the harmonic generator at reduced speed so as to obtain 400 cycles from the seventh harmonic generator and 1200 cycles from an open-delta frequency-tripler.

4. Proposals.

The proposed proceedure was to obtain a complete family of torque-speed curves of the 60 cycle servo motor. Input voltages were to be balanced sinusoids, balanced non-sinusoids, and unbalanced sinusoids. For the 400 cycle motor, it was proposed to impress rated voltage and frequency on the reference winding, and then investigate the effects upon the torque-speed curve when the impressed control winding voltage was (1) of rated rms value at rated frequency, (2) of rated rms value at 1200 cycles, and (3) zero.

5. General precautions.

Early in the investigation it was found that the temperature rise for a given impressed voltage was a function of the slip, and that erratic torque-speed curves were obtained if no effort was made to maintain temperature rise constant. Illustrations 6 and 7 give the torque versus temperature curves of two of the motors tested. Constant casing temperature was controlled as explained in paragraph 2(e) above.

When higher order time-harmonic frequencies were applied to the motor windings, saturation became a problem since the theoretical considerations had assumed no saturation. Saturation, of course, is evidenced by a distortion of the current wave form, consequently, the current wave form was used as the criterion of limiting conditions rather than magnitude and wave shape of impressed voltages. Illustrations 8 and 9 show the current wave form obtained when rated voltage at 1200 cycles was impressed on the control winding and also the current wave forms obtained when the control voltage was decreased to minimize saturation effects.

6. Sinusoidal time-harmonic test-data.

Illustration 10 gives the family of torque-speed curves for rated reference voltage at rated frequency with control voltage at rated frequency as the variable parameter. These curves are typical of those provided by the various manufacturers of servo motors and must be considered normal. It should be noted, however, that these curves would not have been so "typical" had not the casing temperature been maintained substantially constant. Of particular interest in these curves is the linear torque versus control voltage relationship at stall. Illustration 11 is a graphical presentation of this feature. Linearity at stall is of particular importance because of the simplification of interpolation proceedure it affords.

Illustration 12 gives the torque-speed curves for

balanced non-sinusoidal impressed voltages. The fundamental components were made equal to the rated voltage so as to give a more ready comparison with the curves of Illustration 11. A curve of balanced third harmonic voltages of same magnitude as that contained in the approximate rectangular wave is also included in illustration 12. As was predicted by the theoretical analysis, the simulated rectangular voltages produced a torque-speed curve that was - to the accuracy of the recording devices - the difference between the fundamental and third-harmonic torques.

Variation of the phase displacement of the third-time harmonic of the simulated triangular wave had no effect upon the net torque of the complex wave; that is, for a given fundamental and given third harmonic, the net torque was the same for a flat complex wave as for a peaked complex wave.

7. Space-harmonic test data.

The stator winding and rotor of the 400 cycle, Kearfoot motor are shown in illustration 13. The unity pitch factor and unity distribution factor are clearly evident. The variation of gap permeance due to slots and teeth is also clearly shown. From considerations of the stator alone, certainly this motor could have been expected to show the effects of a pronounced third-space harmonic. The test data for this motor, which is presented as the torque-speed curve of illustration 14 nevertheless was smooth. Closer study of the rotor at this time indicated that the skew of the rotor bars

was approximately two-thirds of a pole pitch, or 120° fundamental space degrees. As far as the third-space harmonic is concerned this skew is approximately 360 electrical degrees. The reason for zero third space-harmonic torque is now apparent because the net induced voltage in the rotor resulting from the rotating third-space harmonic of flux in stator must be zero. This design feature would also reduce all higher order space harmonics to negligible magnitudes.

8. Unbalanced time-harmonic test data.

This test was made with maximum undistorted currents in each winding so that the previous theoretical analysis would apply. Distortions at rated current occur because of saturation and transformer action between windings. Illustrations 8 and 9 are oscillograms of the reference and control currents showing how the amount of distortion was decreased by reduction of currents to slightly below rated values.

Before connecting the shaft of the motor to the dynamometer, it was tested under no-load conditions to determine the existence of a torque. It was found that a torque did in fact exist, and that speed could be controlled up to approximately 500 rpm in either direction by variation of the phase displacement of the impressed currents. This of course would tend to refute the previous theoretical analysis; however, after the motor was connected to the dynamometer, the torque-speed curve marked A in illustration 15 was obtained. This is the type of curve one would expect for zero control

voltage. In order to get a comparison with a torque-speed curve for zero impressed control voltage the E_{bb} supply to the amplifier supplying the 1200 cycle voltage was reduced to zero. Curve B of illustration 15 was then obtained, indicating that the 1200 cycle current in the control winding produced no net torque. Curves A and B differ from curve C, which was obtained by shorting the control winding at the motor, because of the additional resistance and inductance introduced in series with the control winding when the secondary of the output transformer is in the motor circuit. Curves A and B are more typical of the zero control voltage curves that would be obtained in a practical application.

A more exacting harmonic analysis of the rated currents was made with the wave analyzer and the following per unit values applying to oscillogram A of illustration 9 were obtained:

cps	400	1200
I_r(ma)	1.000	0.013
I_c(ma)	0.015	1.000

The net developed torque in this instance would be the difference of the 400 and 1200 time harmonic torques, and although this net torque would be extremely small, it would be sufficient to overcome the trifling friction and windage losses of this small motor at these low speeds and thus give the no-load torque previously observed but too small to measure.

In order to determine if these different frequency cur-

rents could produce some higher order space-harmonic rotating field in contradiction to the previously determined theoretical analysis, a solid mild-steel sleeve was shrunk over a spare rotor that had been turned down to below the depth of the rotor slots. The stall torque with this modified rotor was only 33/40 inch ounces as compared to 100/40 inch ounces for the normal rotor when maximum undistorted currents at 400 cycles were forced through both windings. The stall torque for this modified motor was again zero for the 400/1200 cycle test.

9. Appraisal of test data.

Appraisal of the test data discussed above leads to the conclusion that these data are in complete agreement with the theoretical analyses of Chapter II. One additional comment might now be made as a result of the information obtained by test: that is, an a.c. servo motor that has a smooth torque-speed curve for rated voltage and frequency will operate satisfactorily - albeit with higher losses - when the impressed voltages are non-sinusoidal.

CHAPTER IV

CONCLUSIONS

This investigation, in essence, dealt with two separate aspects of the effects upon torque-speed characteristics of typical, production-type servo motors; namely, the effect of time harmonics and the effect of space harmonics. First through a theoretical analysis of certain proposed conditions, and then through an experimental analysis of these same conditions, it was shown that the conclusions to be drawn from either approach agreed remarkably well with the other. These conclusions may be summarized as follows:

1) Distorted or complex wave forms of impressed voltage will reduce net developed torque for a given temperature rise of the motor, but this reduction will rarely - if ever - exceed 30 percent in practice. This reduced net torque is due to the relative reduction in magnitude of the sinusoidal component of fundamental frequency plus the negative torques developed by the third and seventh time harmonics.

2) Variation of the winding temperature within the limits of ambient and maximum allowable temperature rise could well have the greatest effect upon the smoothness of the torque-speed characteristic of all the operating conditions investigated.

3) The effect of the third-space harmonic must be eliminated by proper application of available design tech-

niques before any two-phase servo motor may be termed usable as regards application to feed-back control circuits.

4) A most satisfactory criterion of adequacy of design safeguards against possible adverse effects upon the desired operating characteristics of a given servo motor due to complex impressed voltages is the smoothness of the torque-speed curve throughout the entire range of plus and minus synchronous speed.

5) In general, the adverse effects of complex impressed voltage wave forms that can be expected in practice need not seriously limit the application of the modern production-type two-phase servo motor.

BIBLIOGRAPHY

1. Alger, P. L.	The Nature of Polyphase Induction Machines, John Wiley & Sons, 1951
2. Behrend, B.A.	The Induction Motor, 2nd Edition, Mcgraw - Hill, 1921
3. Churchill, R.V.	Fourier Series and Boundary Value Problems, McGraw - Hill, 1941
4. Dreese, E. E.	Synchronous Motor Effects in Induction Machines, AIEE Transactions, Vol. 49, pp 1033-1042, July, 1930.
5. Gray, T. S.	Applied Electronics, 2nd Edition, John Wiley and Sons, 1954 - p 378
6. Kerchner, R.M. and Corcoran, G.F.	Alternating Current Circuits, 3rd Edition, John Wiley and Sons, 1951
7. Koopman, R.J.W.	Operating Characteristics of Two Phase Servo Motors, AIEE Transactions, Vol. 68, Part 1, pp 319-327, 1949
8. Kron, G.	Induction Motor Slot Combinations, AIEE Transactions, Vol. ~~49~~ 50, pp 757-768, ~~July~~ June 1931
9. Lawrence, R.R. and Richards, H.E.	Principles of Alternating-Current Machinery, 4th Edition, Mcgraw-Hill, 1953
10. Puchstein, A.F. and Lloyd, T.C.	Alternating-Current Machines, 2nd Edition, John Wiley and Sons, 1949
11. Stein, W. A.	The Determination of Rotor Inductance and Resistance for a Drag Cup Servomotor, AIEE Conference Paper, April 1953
12. Thaler, G.J. and Brown, R.G.	Servomechanism Analysis, McGraw - Hill, 1953
13. Van Wambeck, S.K. and Stein, W.A.	A Special Dynamometer for testing Small Motors, AIEE Transactions, Vol. 71, pp 549-553, June 1952

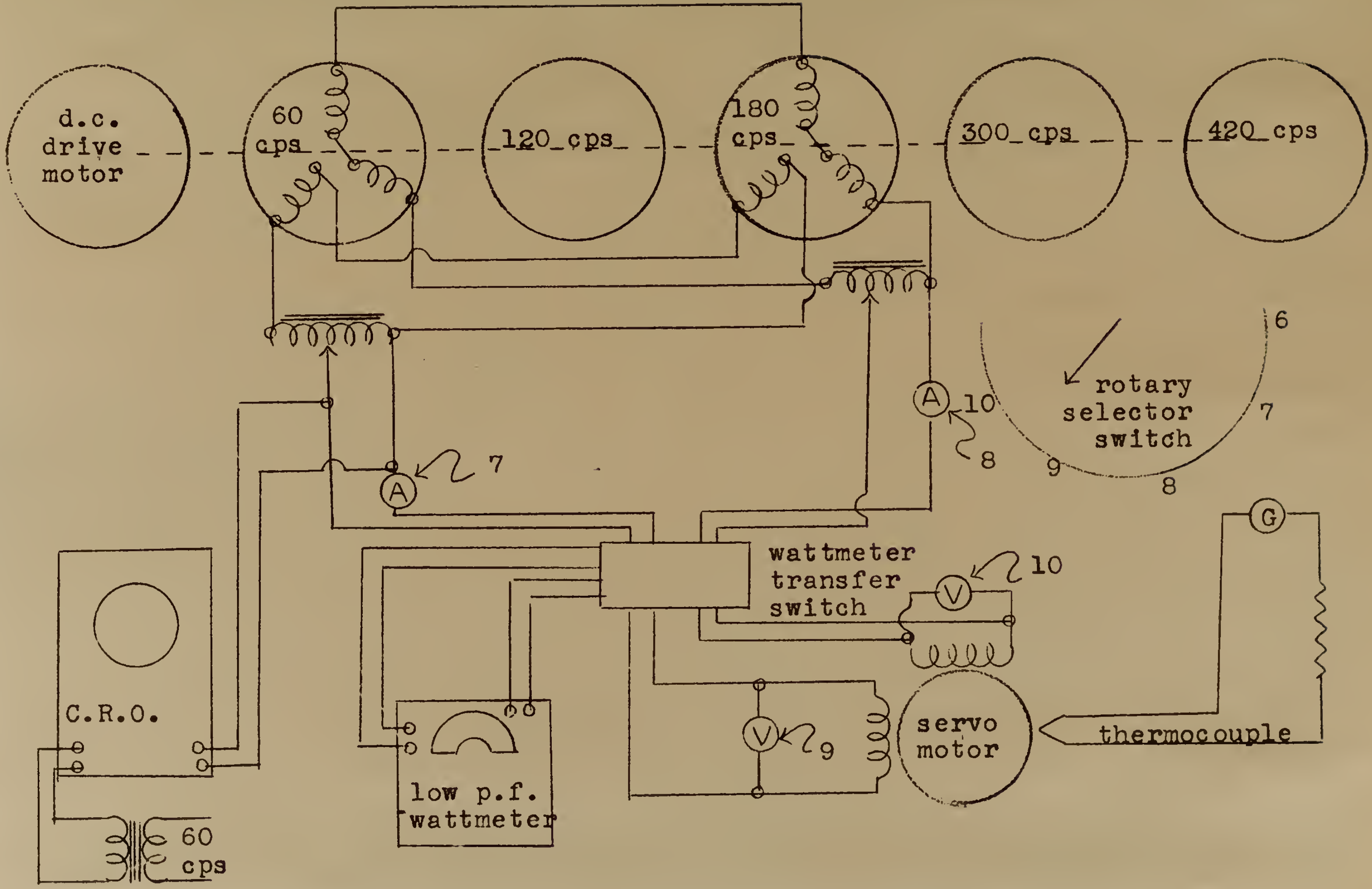

Schematic diagram of circuitry for early phases of investigation.

ILLUSTRATION 1

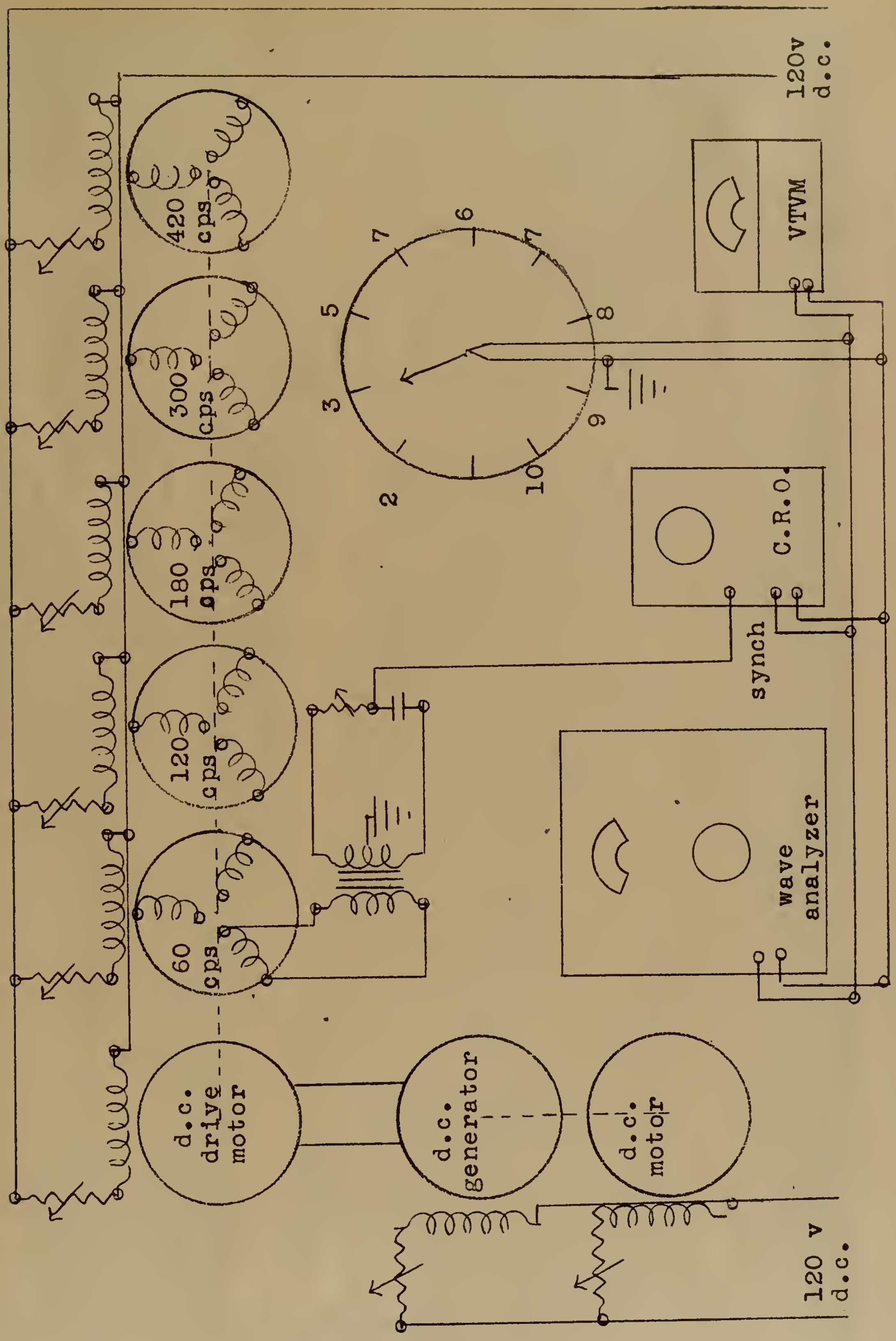

Schematic diagram of frequency control and oscilloscope triggering circuits.

ILLUSTRATION 2

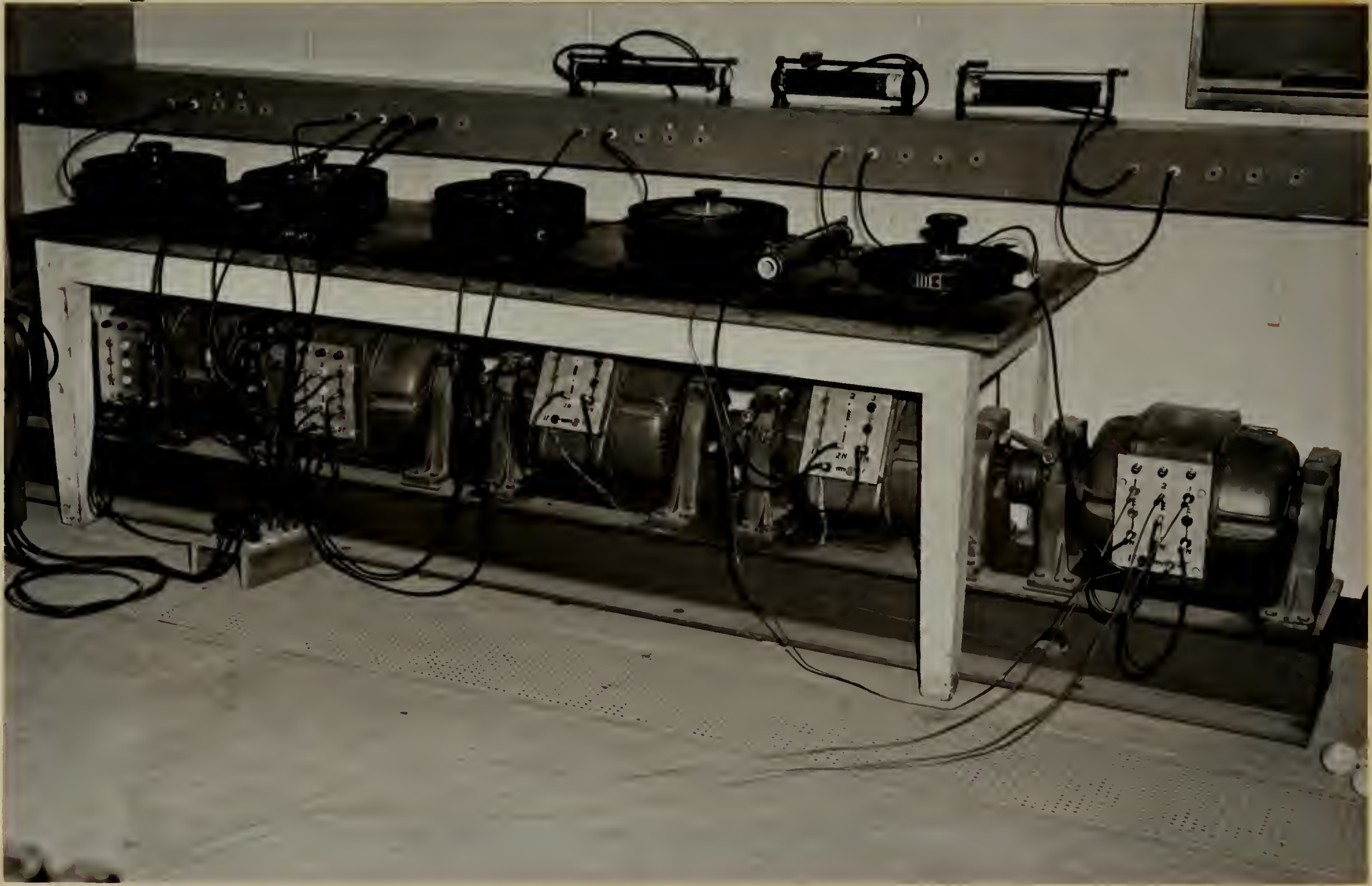

ILLUSTRATION 3: Photograph of harmonic generator

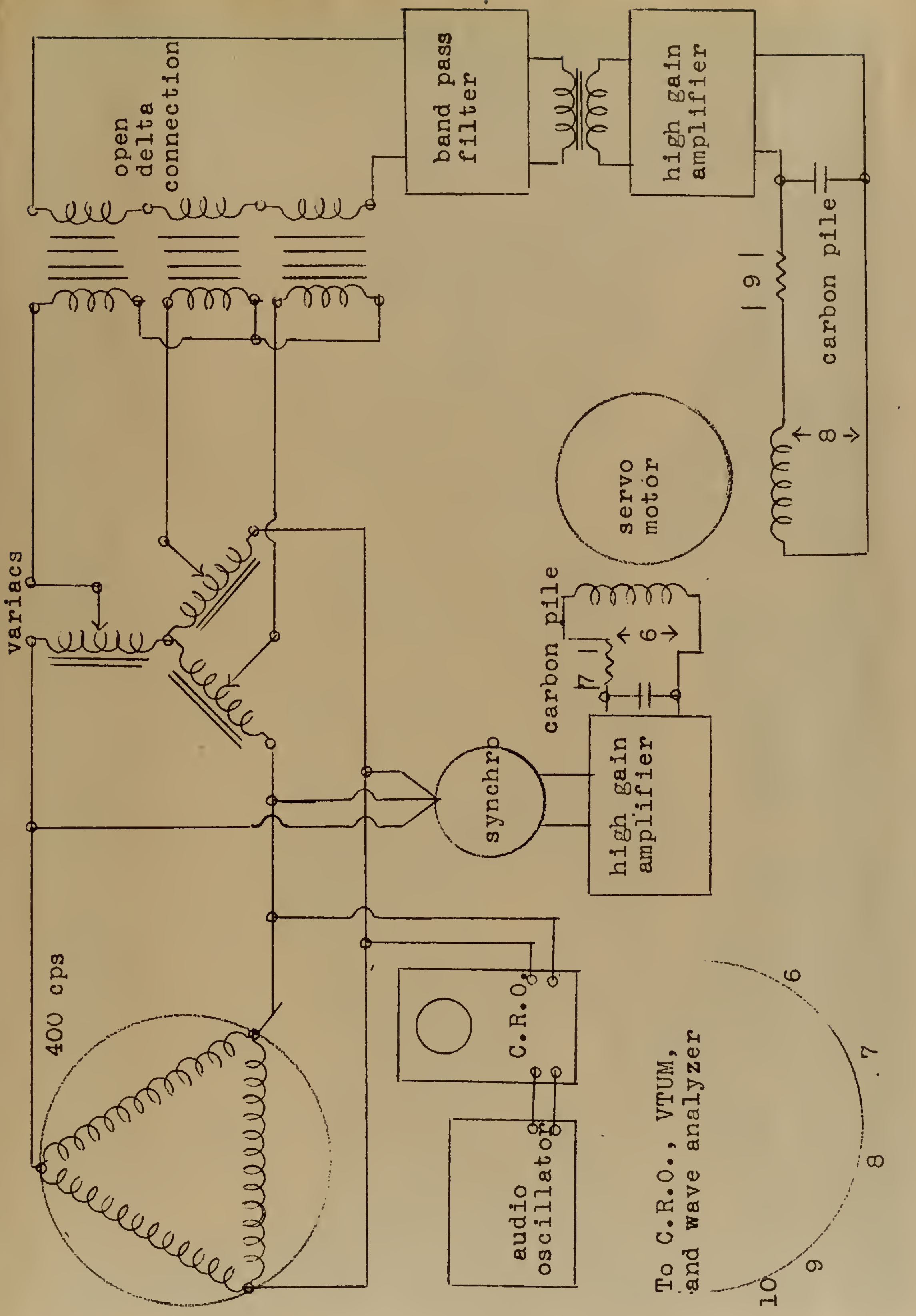

Frequency tripler circuit

ILLUSTRATION 4

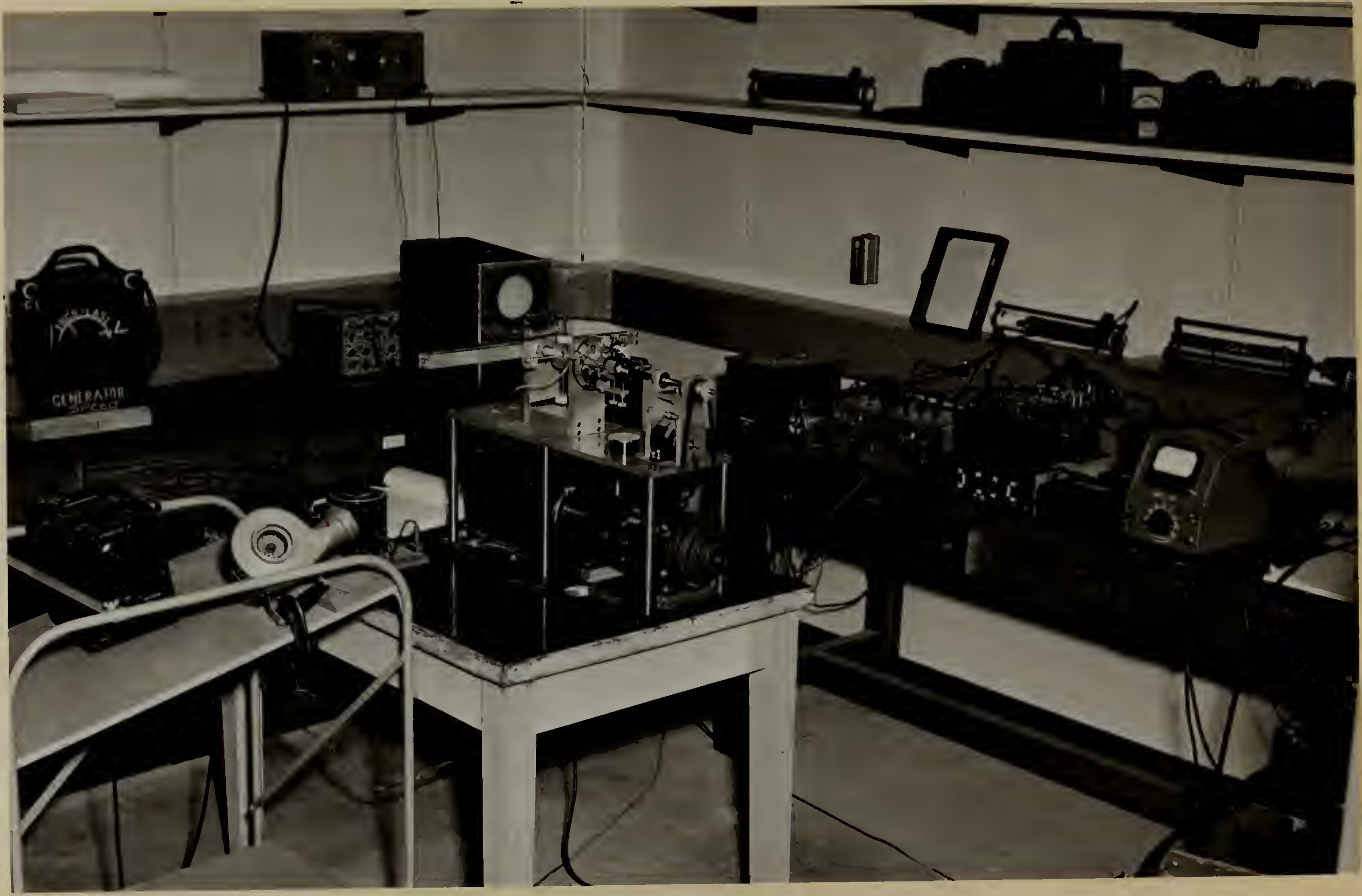

ILLUSTRATION 5: Photograph of dynamometer and temperature control

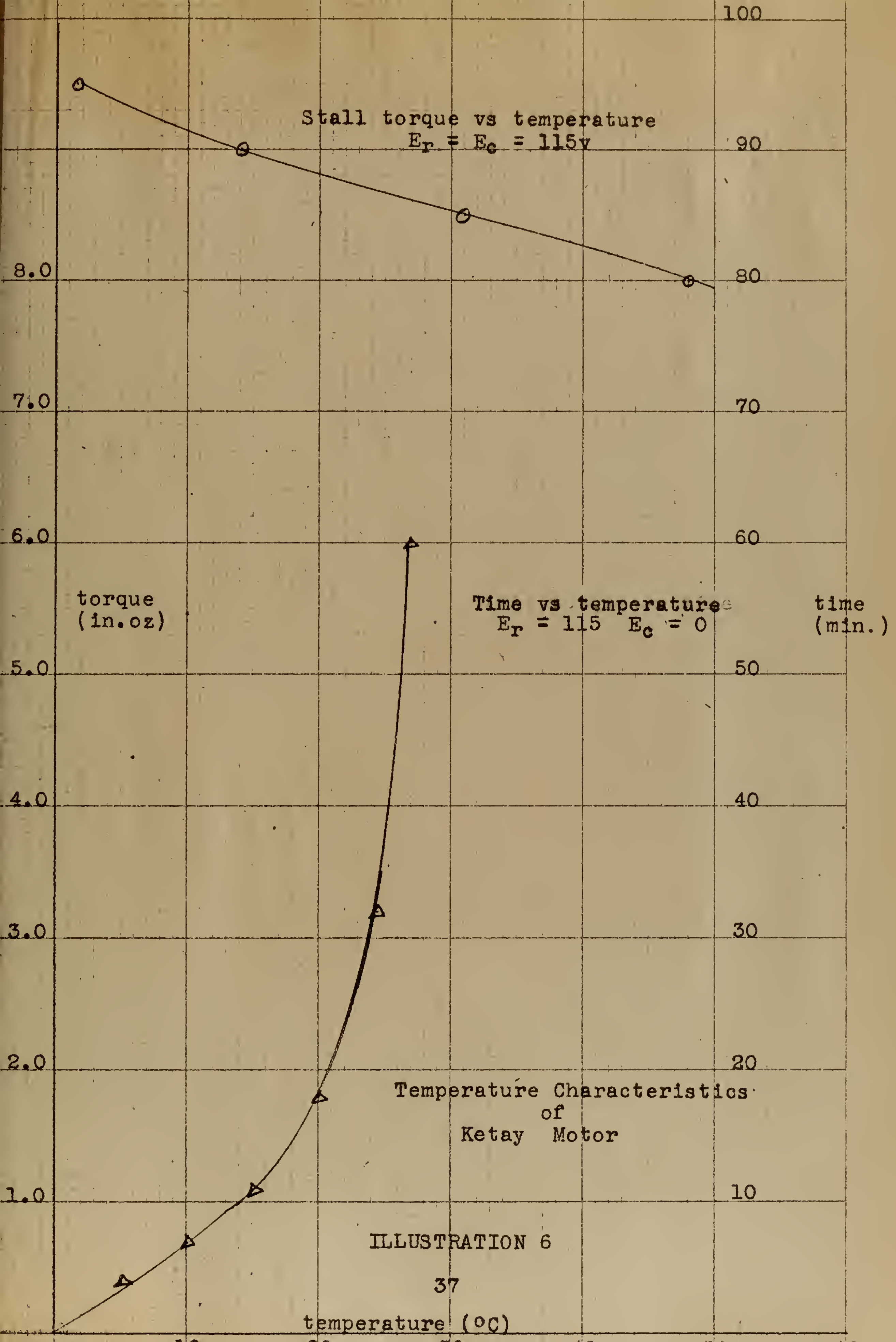

Temperature Characteristics
of
Ketay Motor

ILLUSTRATION 6

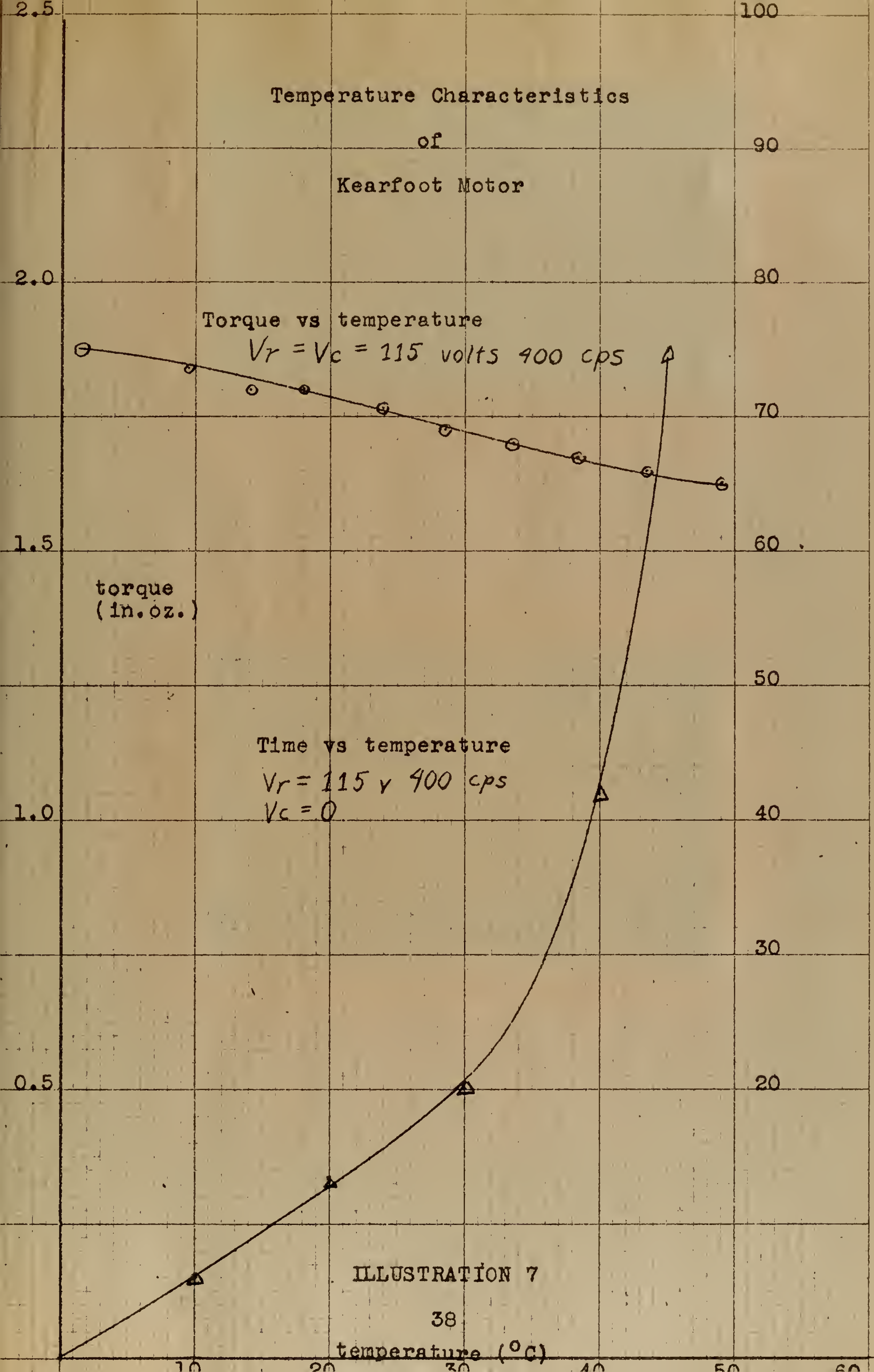
Temperature Characteristics
of
Kearfoot Motor

ILLUSTRATION 7

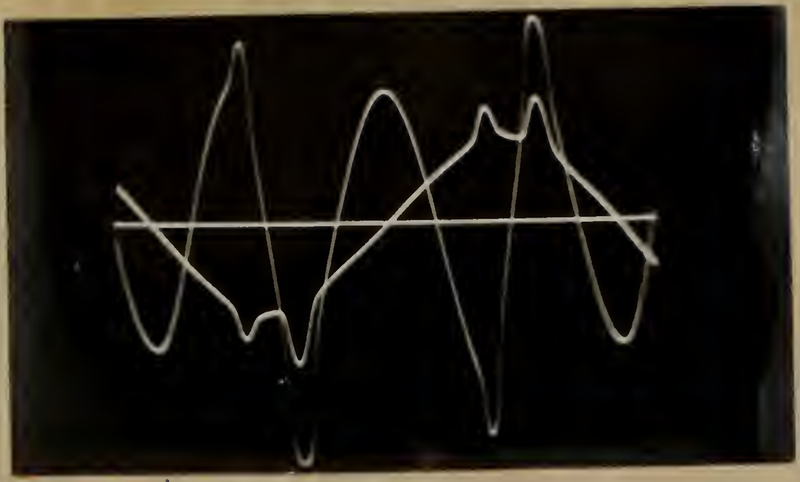

(a)

cps	400	1200	2000	2800	3600
I_r (ma)	245	16	14	20	16
I_c (ma)	18	495	110	42	34

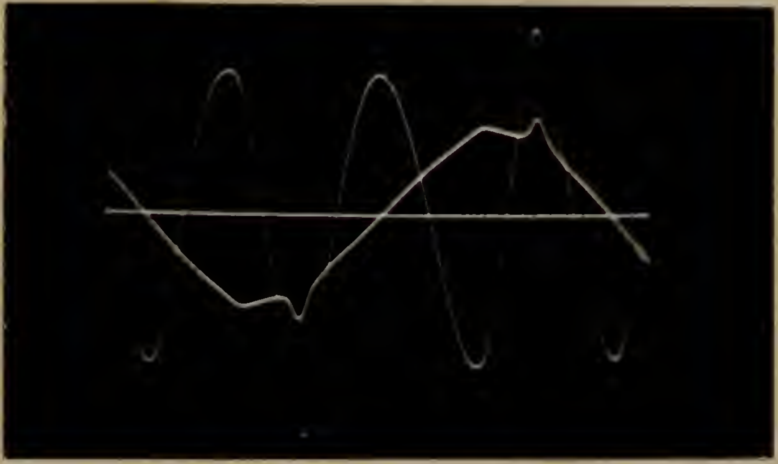

(b)

cps	400	1200	2000	2800	3600
I_r (ma)	225	7	7	10	6
I_c (ma)	17	445	60	21	21

Current oscillograms showing effects of saturation for 400/1200 cps investigation.

ILLUSTRATION 8

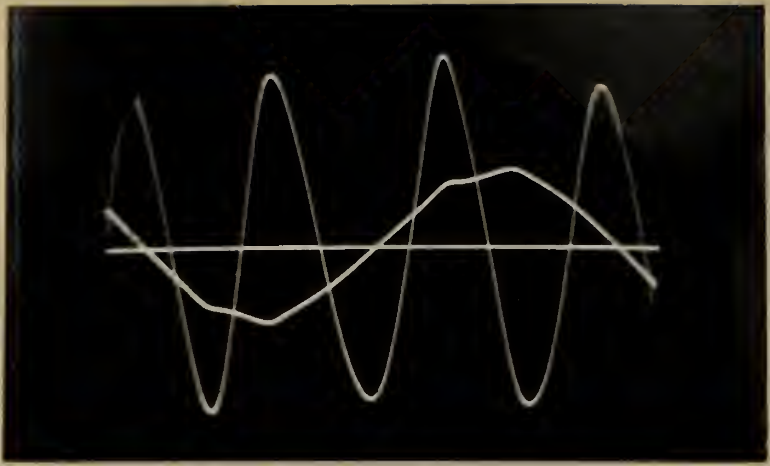

(a)

cps	400	1200	2000	2800	3600
I_r (ma)	195	2.5	2.5	1.9	0.8
I_c	5.4	370	19	2.3	7.0

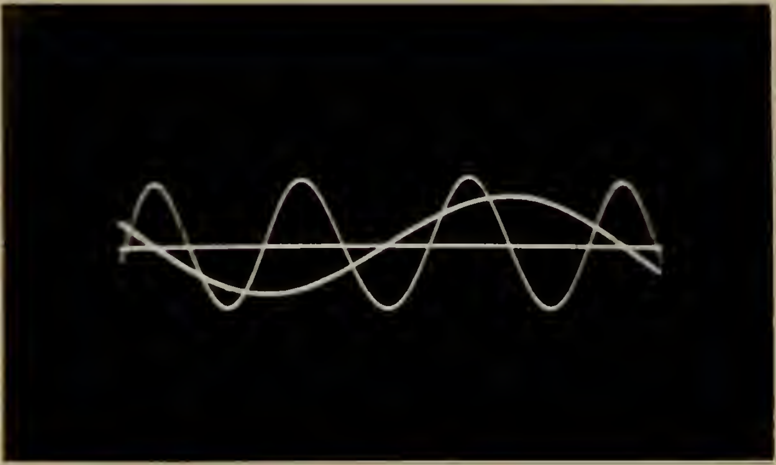

(b)

cps	400	1200	2000	2800	3600
I_r (ma)	150	1.0	0.7	0.4	0.1
I_c (ma)	1.8	200	3.4	0.5	2.0

Current oscillograms of rated and sub-rated currents for 400/1200 cps investigation

ILLUSTRATION 9

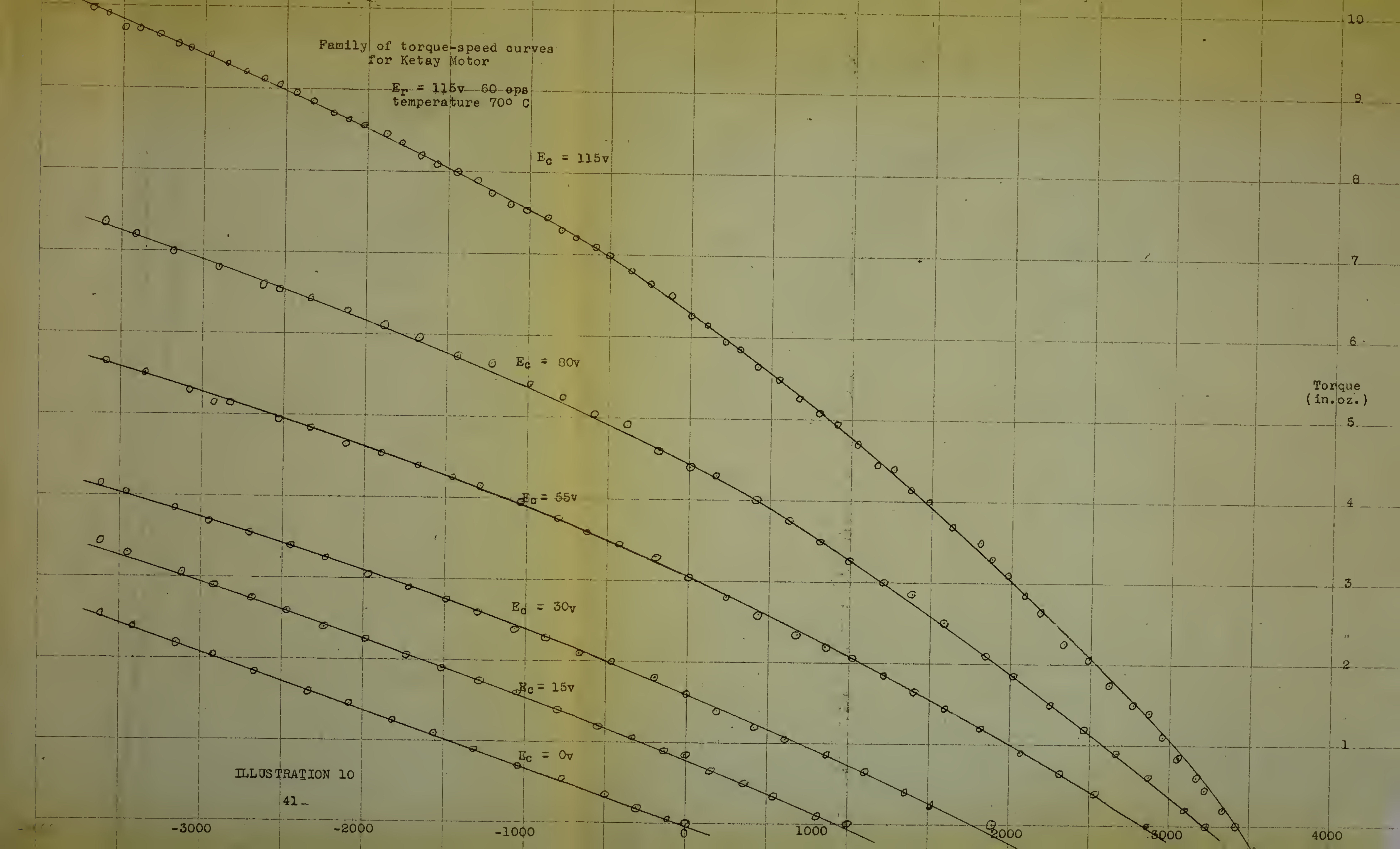

ILLUSTRATION 10

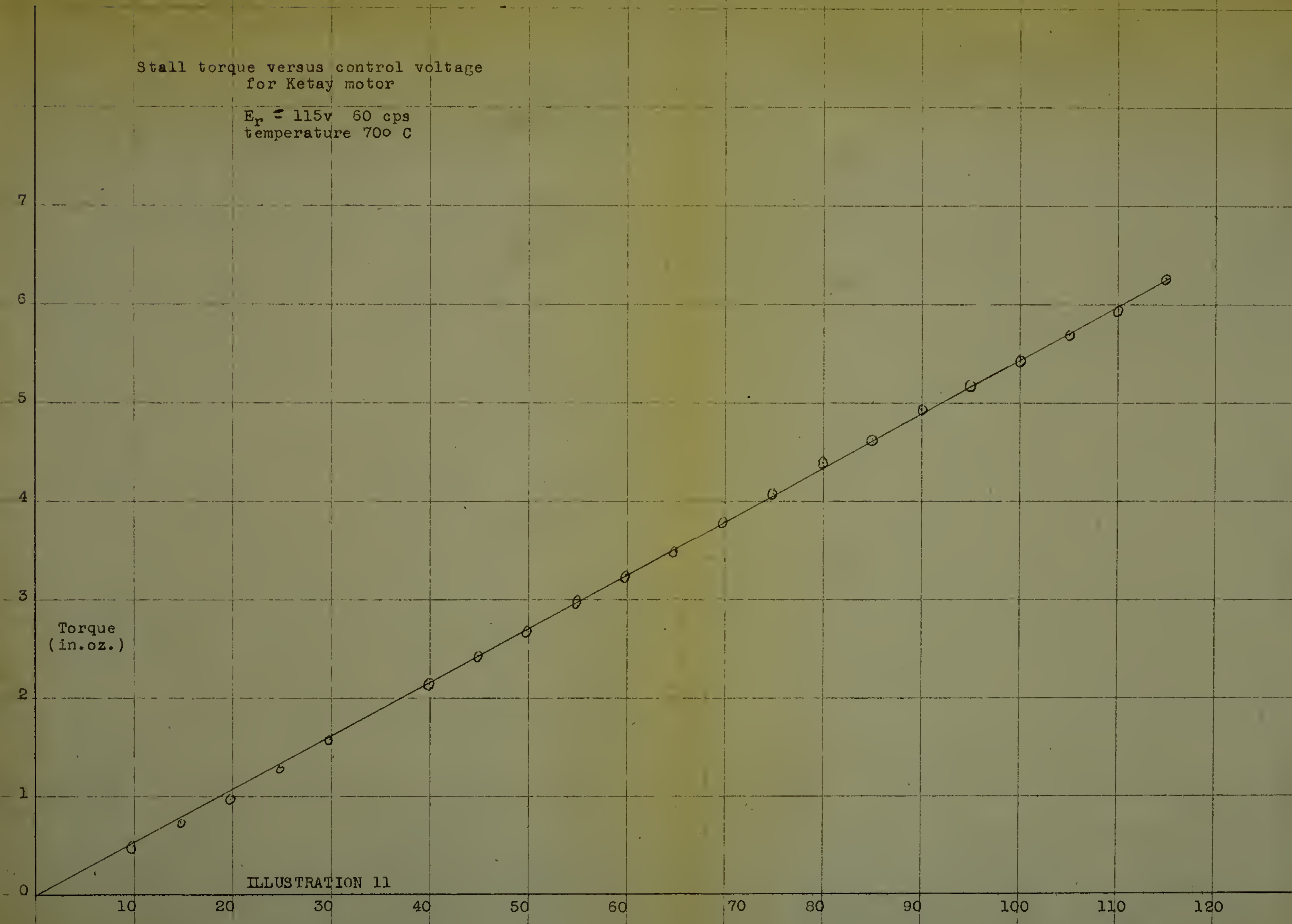

ILLUSTRATION 11

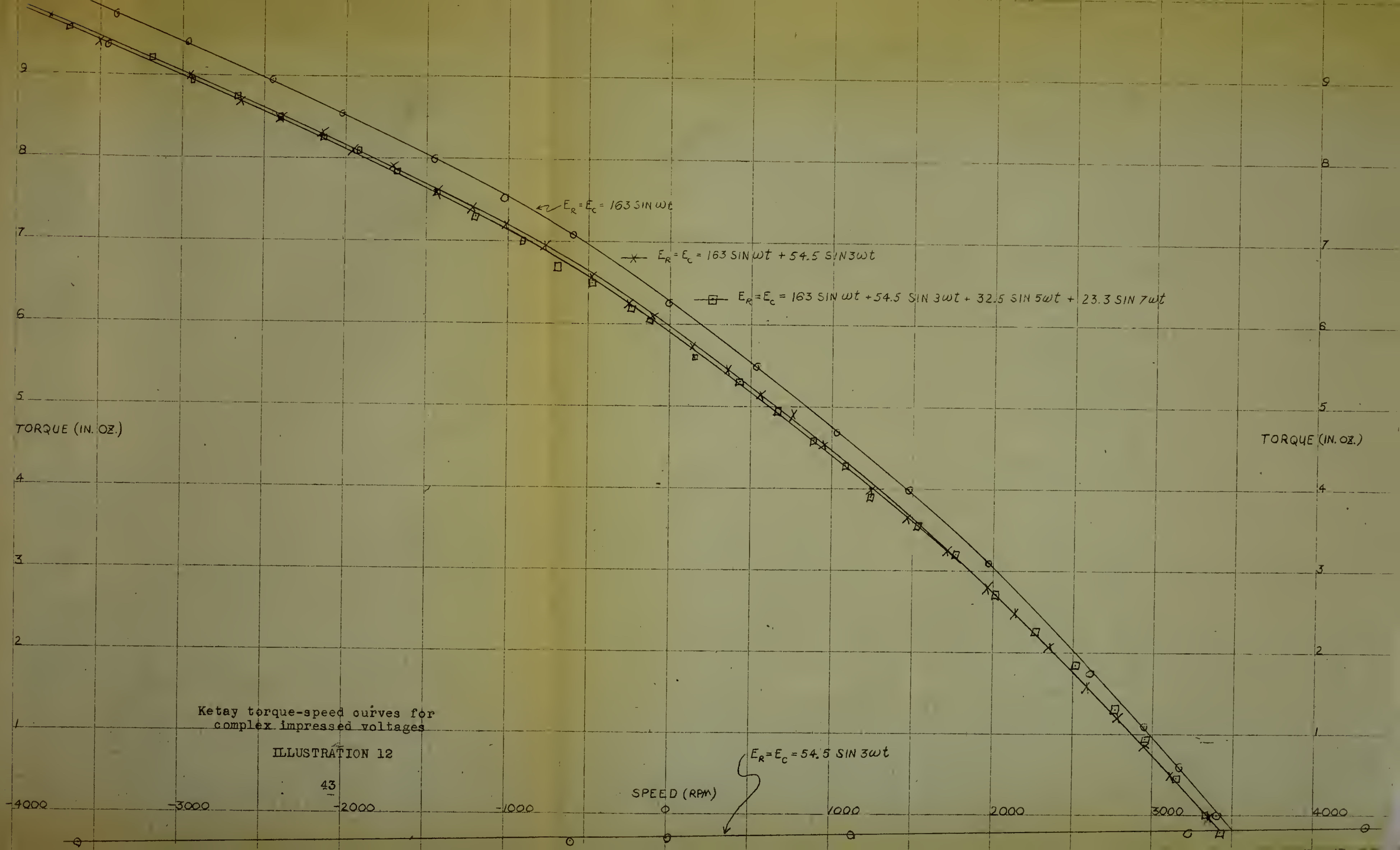

Ketay torque-speed curves for complex impressed voltages

ILLUSTRATION 12

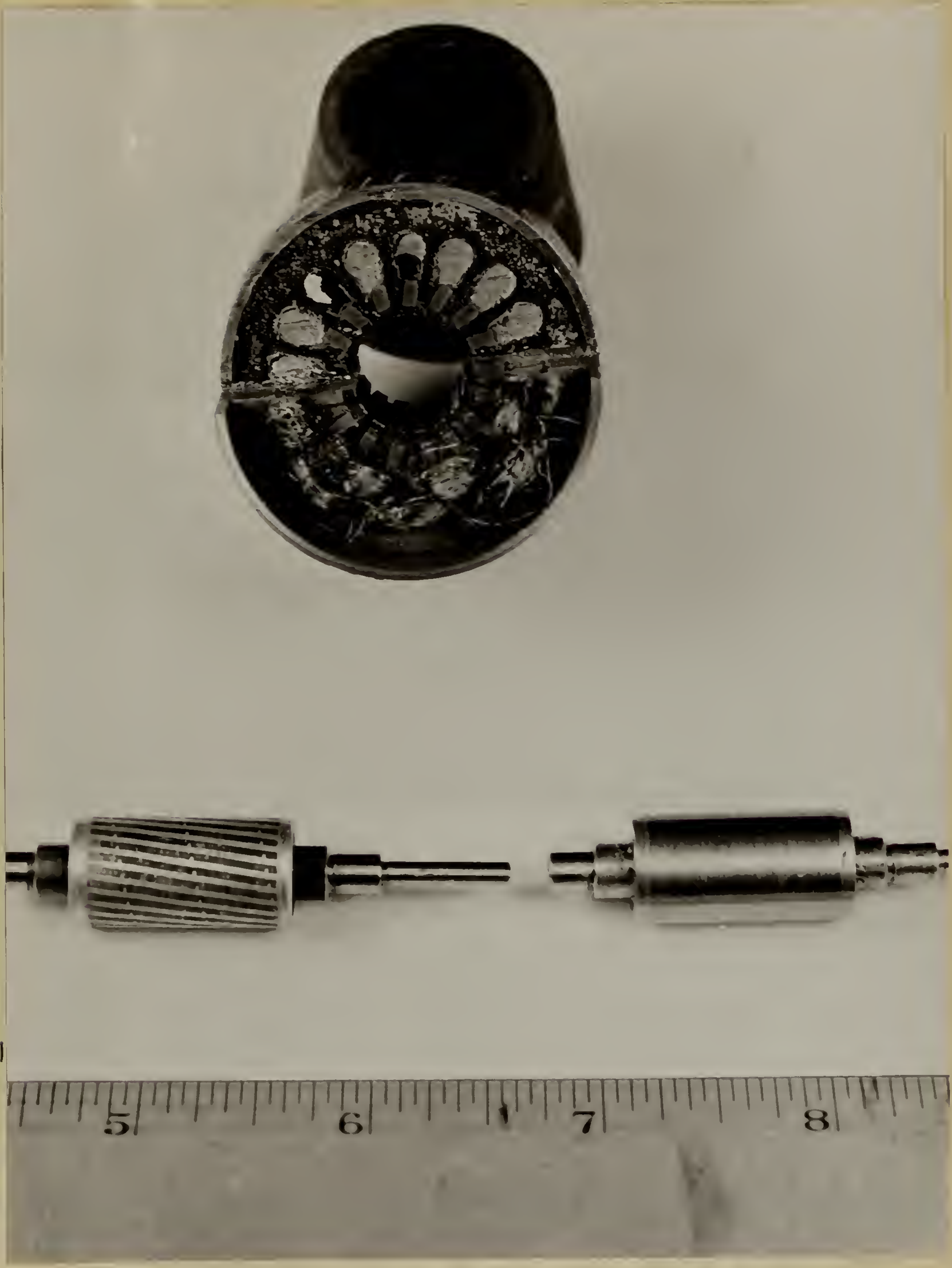

Cutaway photograph of Kearfoot motor

ILLUSTRATION 13

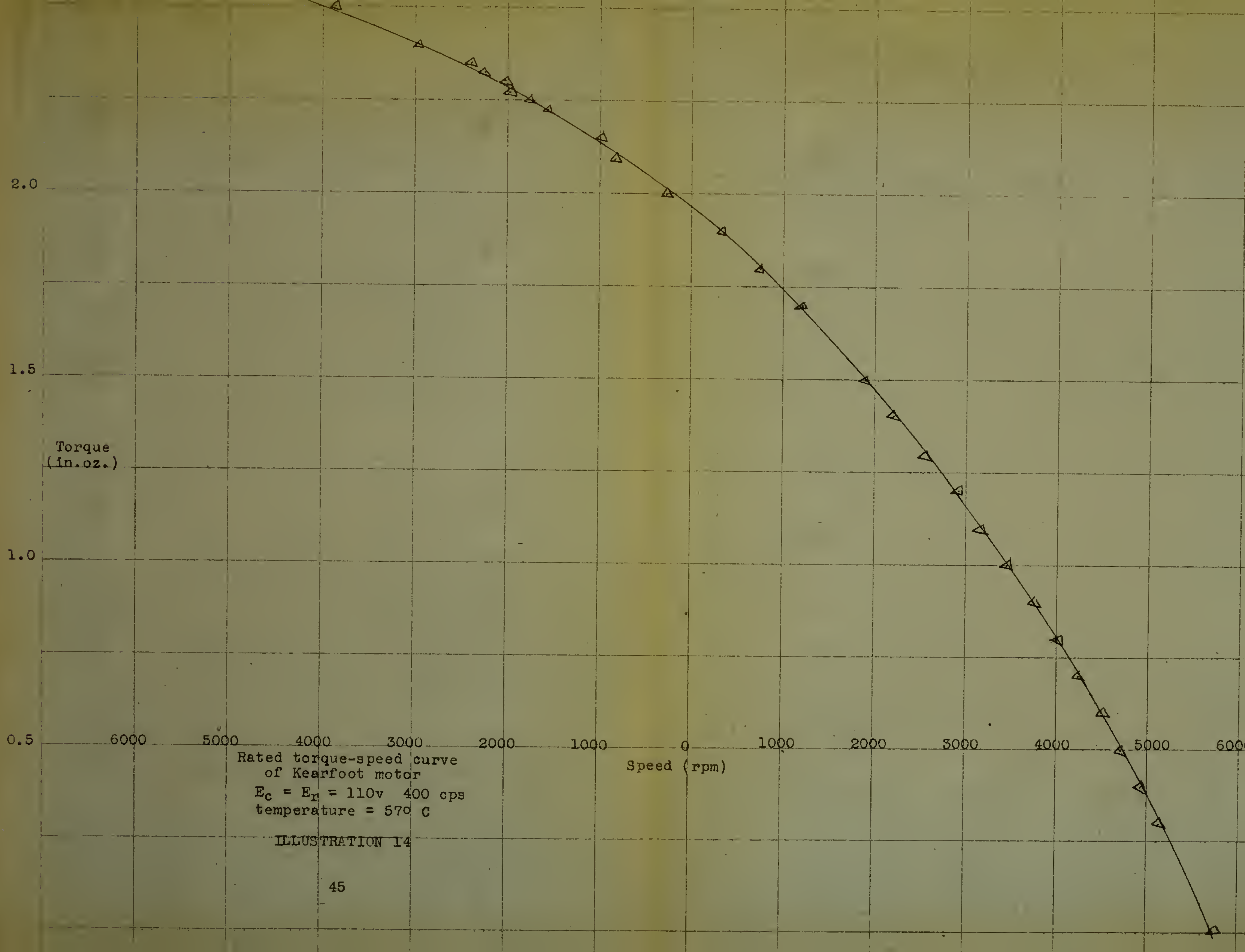

Rated torque-speed curve
of Kearfoot motor
$E_c = E_r = 110$v 400 cps
temperature = 57° C

ILLUSTRATION 14

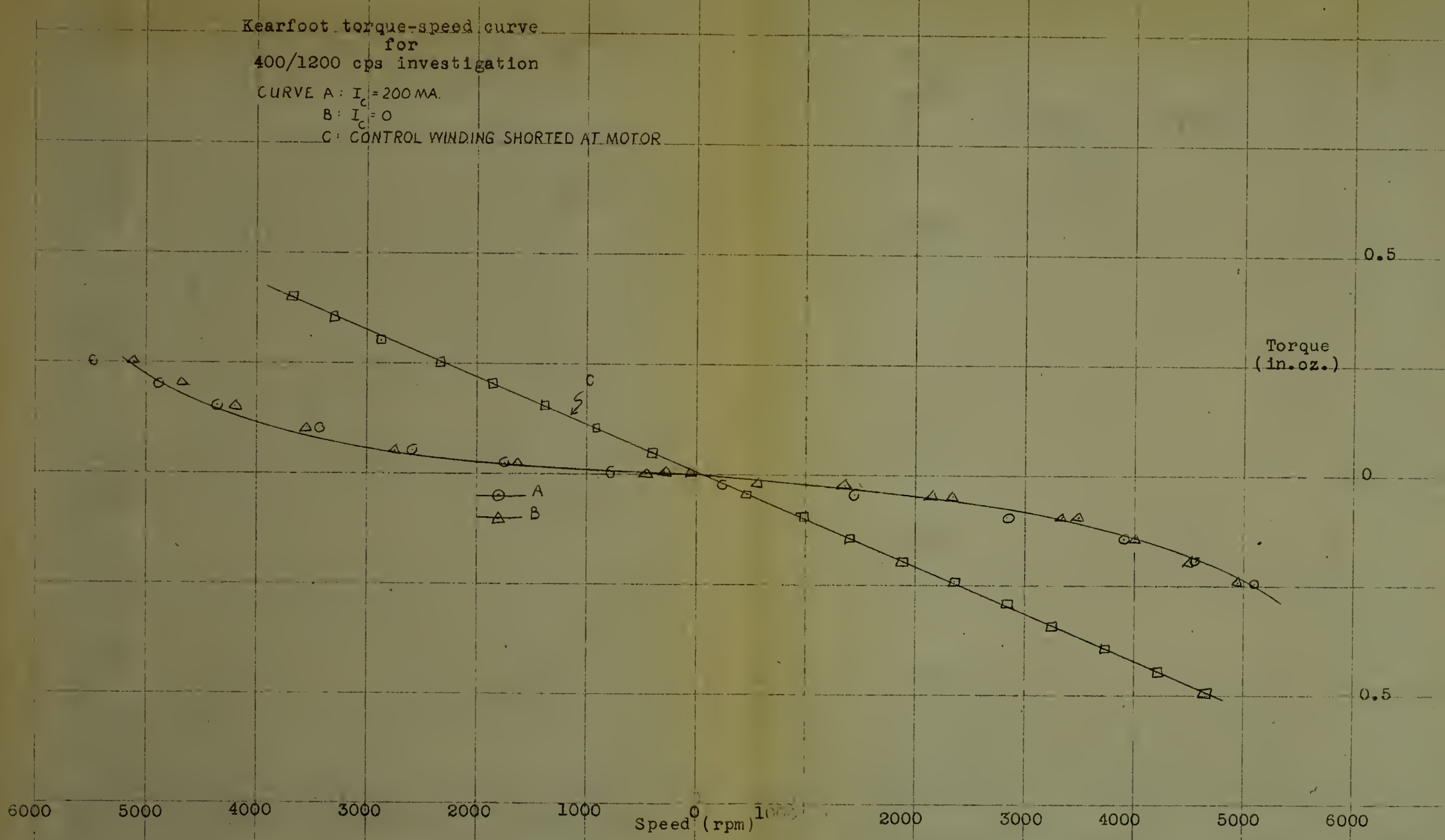

Kearfoot torque-speed curve
for
400/1200 cps investigation

ILLUSTRATION 15

Schematic diagram of wattmeter transfer switch (8P-DT snap sw.)

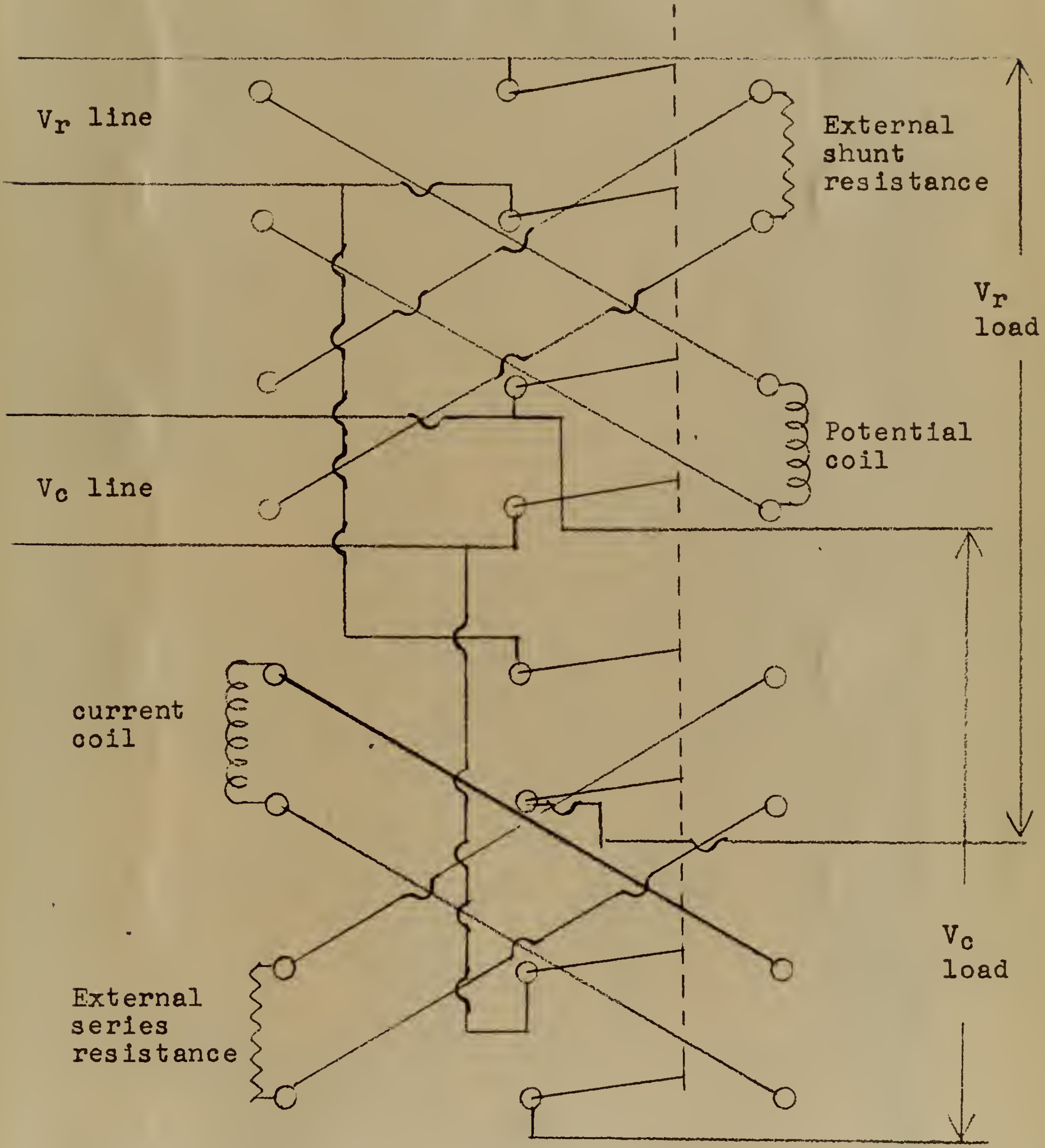

ILLUSTRATION 16

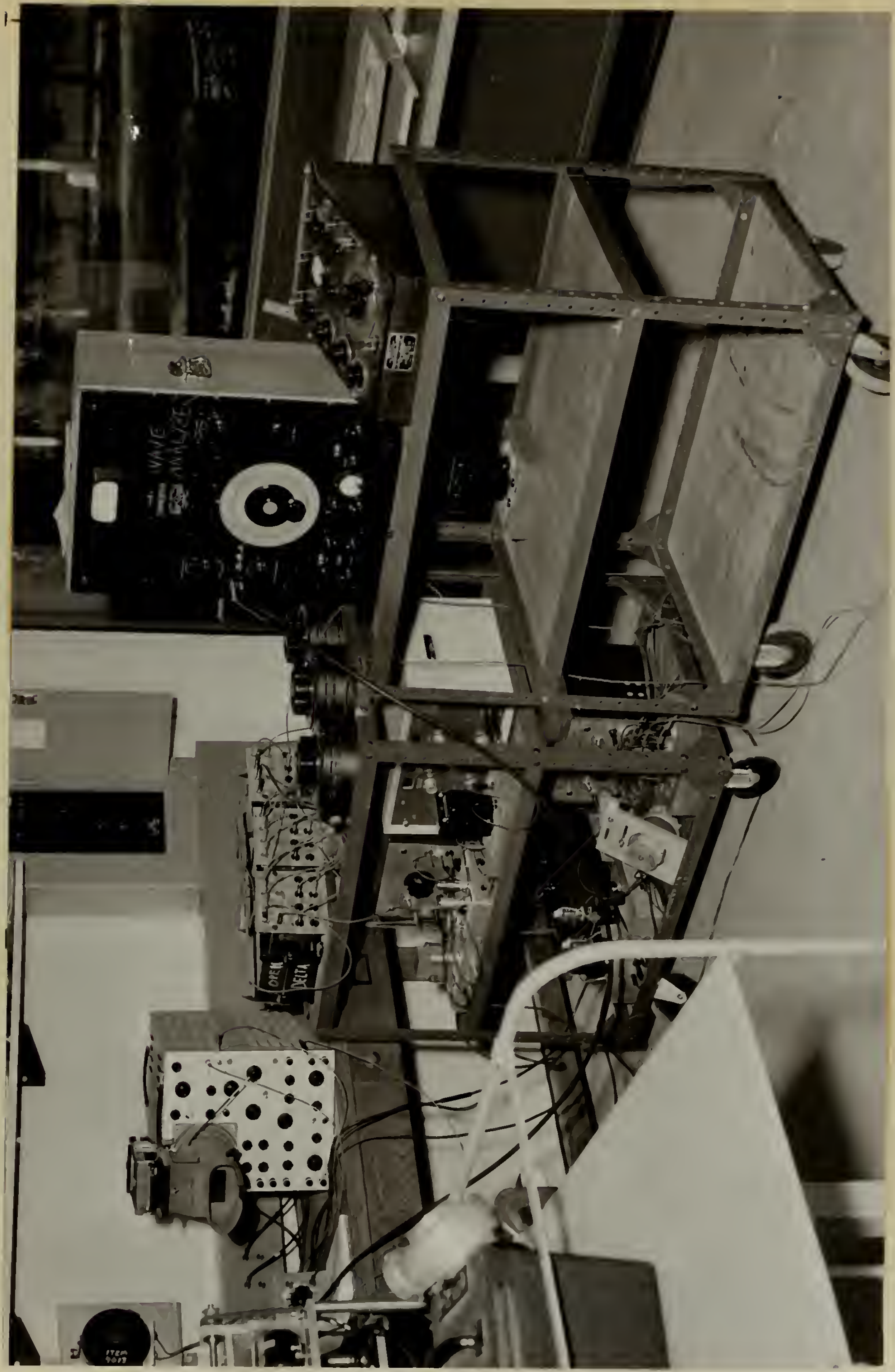

ILLUSTRATION 17: Photograph of frequency tripler set-up

SE 958
SE 958
FE 20 63
4922
8487

Thesis
B92 Busey
28483
The effect of non-sinusoidal impressed voltages on A.C. servo motors.

SE 958
SE 958
FE 20 63
4922
8487

Thesis
28483
B92 Busey
The effect of non-sinusoidal impressed voltages on A.C. servo motors.

thesB92
The effect of non-sinusoidal impressed v
3 2768 002 08823 9
DUDLEY KNOX LIBRARY